

The Kolmogorov Superposition Theorem can Break the Curse of Dimension When Approximating High Dimensional Functions

Ming-Jun Lai*

Zhaiming Shen[†]

December 3, 2024

Abstract

We explain how to use Kolmogorov Superposition Theorem (KST) to break the curse of dimensionality when approximating a dense class of multivariate continuous functions. We first show that there is a class of functions called Kolmogorov-Lipschitz (KL) continuous in $C([0, 1]^d)$ which can be approximated by a special ReLU neural network of two hidden layers with a dimension independent approximation rate $O(1/n)$ with approximation constant increasing quadratically in d . The number of parameters used in such neural network approximation equals to $(6d + 2)n$. Next we introduce KB-splines by using linear B-splines to replace the outer function and smooth the KB-splines to have the so-called LKB-splines as the basis for approximation. Our numerical evidence shows that the curse of dimensionality is broken in the following sense: When using the standard discrete least squares (DLS) method to approximate a continuous function, there exists a pivotal set of points in $[0, 1]^d$ with size at most $O(nd)$ such that the rooted mean squares error (RMSE) from the DLS based on the pivotal set is similar to the RMSE of the DLS based on the original set with size $O(n^d)$. The pivotal point set is chosen by using matrix cross approximation technique and the number of LKB-splines used for approximation is the same as the size of the pivotal data set. Therefore, we do not need too many basis functions as well as too many function values to approximate a high dimensional continuous function f .

Key words: Kolmogorov Superposition Theorem, Functions Approximation, B-splines, Multivariate Splines Denoising, Sparse Solution, Pivotal Point Set

AMS Subject Classification: 41A15, 41A63, 15A23

1 Introduction

Recently, deep learning algorithms have shown a great success in many fronts of research, from image analysis, audio analysis, biological data analysis, to name a few. Incredibly, after a deep learning training of thousands of images, a computer can tell if a given image is a cat, or a dog, or neither of them with very reasonable accuracy. In addition, there are plenty of successful stories such that deep learning algorithms can sharpen, denoise, enhance an image after an intensive training. See, e.g. [24] and [51]. The 3D structure of a DNA can be predicted very accurately by using the DL approach. The main ingredient in DL algorithms is the neural network approximation based on ReLU functions. We refer to [11] and [13] for detailed explanation of the neural network approximation in deep learning algorithms and the literature therein.

*mjlai@uga.edu. Department of Mathematics, University of Georgia, Athens, GA 30602. This author is supported by the Simons Foundation Collaboration Grant #864439.

[†]zshen49@gatech.edu. School of Mathematics, Georgia Institute of Technology, Atlanta, GA 30332.

Learning a multi-dimensional data set is like approximating a multivariate function. The computation of a good approximation suffers from the curse of dimension. For example, suppose that $f \in C([0, 1]^d)$ with $d \gg 1$. One usually uses Weierstrass theorem to have a polynomial P_f of degree n such that

$$\|f - P_f\|_\infty \leq \epsilon$$

for any given tolerance $\epsilon > 0$. As the dimension of polynomial space $= \binom{n+d}{n} \approx n^d$ when $n > d$, one will need at least $N = O(n^d)$ data points in $[0, 1]^d$ to distinguish different polynomials in \mathbb{P}_n and hence, to determine this P_f . Notice that many good approximation schemes enable P_f to approximate f at the rate of $O((1/n)^m)$ if f is of m times differentiable. In terms of the number N of data points which should be greater than or equal to the dimension of polynomial space \mathbb{P}_n , i.e. $N \geq n^d$, the order of approximation is $O(1/(N^{1/d})^m)$. When $d \gg 1$ is bigger, the order of approximation is less. This phenomenon is the well-known curse of dimensionality. Sometimes, such a computation is also called intractable.

Similarly, if one uses a tensor product of B-spline functions to approximate $f \in C([0, 1]^d)$, one needs to subdivide the $[0, 1]^d$ into n^d small subcubes by hyperplanes parallel to the axis planes. As over each small subcube, the spline approximation S_f of f is a polynomial of degree k , e.g., $k = 3$ if the tensor product of cubic splines are used. Even with the smoothness, one needs $N = O(k^d)$ data points and function values at these data points in order to determine a polynomial piece of S_f over each subcube. Hence, over all subcubes, one needs $O(n^d k^d)$. It is known that the order of approximation of S_f is $O(1/n^{k+1})$ if f is of $k + 1$ times coordinatewise differentiable. In terms of $N = O(n^d k^d)$ points over $[0, 1]^d$, the approximation order of S_f will be $O(k^{k+1}/N^{(k+1)/d})$. More precisely, in [12], the researchers showed that the approximation order $O(1/N^{1/d})$ can not be improved for smooth functions in Sobolev space $W^{k,p}$ with L_p norm ≤ 1 . In other words, the approximation problem by using multivariate polynomials or by tensor product B-splines is intractable.

Furthermore, many researchers have worked on using ridge functions, deep neural networks, and ReLU and many newly invented activation functions to approximate functions in high dimension. See [49, 57, 58, 3] for detailed statements and proofs. More recently, the super approximation power was introduced in [64] which uses the floor function, exponential function, step function, and their compositions as the activation function and can achieve the exponential approximation rate. Although the number of the depth and the number of the width of deep neural networks are quadratically dependent on the dimensionality $d \geq 2$ (cf. [65]), any training of such a neural network requires an exponentially many data locations and function values. That is, the approximation problem by using these neural networks is intractable.

Let us summarize the bottleneck problem of approximating high dimensional functions as follows. The curse of dimensionality (COD) contains three difficult components: (1) one has to use exponentially many basis functions when approximating a high dimensional function; (2) one has to use exponentially many function values from the function to be approximated; and (3) the rate of convergence decreases to zero as $d \rightarrow \infty$. In particular, it is hard or very expensive to obtain an exponential amount of high dimensional data (points and functions). Such an amount of data is even too much for the current computer storage.

However, there is a way to overcome the curse of dimensionality as explained by Barron in [4]. Let $\Gamma_{B,C}$ be the class of functions f defined over $B = \{\mathbf{x} \in \mathbb{R}^d, \|\mathbf{x}\| \leq 1\}$ such that $C_f \leq C$, where C_f is defined as follows:

$$C_f = \int_{\mathbb{R}^d} |\omega| |\tilde{f}(\omega)| d\omega$$

with $|\omega| = (\omega \cdot \omega)^{1/2}$ and \tilde{f} is the Fourier transform of f .

Theorem 1 (Barron, 1993) *For every function f in $\Gamma_{B,C}$, every sigmoidal function ϕ , every probability measure μ , and every $n \geq 1$, there exists a linear combination of sigmoidal functions $f_n(x)$, a shallow neural network, such that*

$$\int_B (f(\mathbf{x}) - f_n(\mathbf{x}))^2 d\mu(\mathbf{x}) \leq \frac{(2C)^2}{n}. \quad (1)$$

The coefficients of the linear combination in f_n may be restricted to satisfy $\sum_{k=1}^n |c_k| \leq 2C$, and $c_0 = f(0)$.

The Barron result shows that there exists an approximation scheme which only needs n terms of sigmoidal functions f_n and achieves the order $O(1/n)$ independent of d . However, it does not know how to obtain this approximation scheme without using an exponentially many data values. It is worth noting that although the approximation rate is independent of the dimension in the L_2 norm sense, the constant C can be exponentially large in the worst case scenario as pointed out in [4]. This work leads to many recent studies on the properties and structures of Barron space $\Gamma_{B,C}$ and its extensions, e.g. the spectral Barron spaces and the generalization using ReLU or other more advanced activation functions instead of sigmoidal functions above, e.g., [32], [15], [16], [17], [18], [66], [67], and the references therein. However, how to achieve the rate of convergence in (1) is still under study.

For practical purposes, to overcome the curse of dimensionality, let us use the following definition.

Definition 1 *Fix a discrete semi-norm of interest, e.g. $\|f\|_{\mathcal{P}} = \sqrt{\sum_{i=1}^N (f(\mathbf{x}_i))^2/N}$, where $\mathbf{x}_i, i = 1, \dots, N$ are points in $[0, 1]^d$. When approximating a continuous function $f \in C([0, 1]^d)$, if there is a scheme S_n based on $O(nd)$ basis functions and function values $f(\mathbf{x}_i), i = 1, \dots, O(nd)$ with $\mathbf{x}_i \in [0, 1]^d$ such that the error $\|f - S_n\|_{\mathcal{P}\mathcal{P}} \leq C(1/n^\alpha)$ for a positive number α independent of d , and a positive constant C which may be dependent on d quadratically and dependent on f , but independent of n , then we say the scheme S_n does not suffer from the curse of dimensionality, where $\|\cdot\|_{\mathcal{P}\mathcal{P}}$ is another discrete semi-norm based on a much denser points than the points \mathbf{x}_i 's in $[0, 1]^d$.*

Let us comment that the number of data (points and function values) has to be dependent on the dimensionality. For example, to approximate a linear polynomial p in d -dimensional space, we need $(d + 1)$ points and its values in order to have a good approximation in general. Also, function f can grow very quickly as and/or oscillate very quickly $d \rightarrow \infty$. There are no way to use such a small number of data (points and function values), i.e. $O(nd)$ samples of the values of a function $f(\mathbf{x}) = \|\mathbf{x}\|^{d^d}$ to approximate it. Thus, we have to restrict ourselves to some classes of functions which are bounded and/or oscillate grow moderately. These will be more precisely described later in the paper.

In this paper, we turn our attention to Kolmogorov superposition theorem (KST) and will see how it plays a role in the study how to approximate high dimensional continuous function and how it can be used to break the curse of dimensionality when approximating high dimensional functions which grows and/or oscillate moderately for $d = 2, 3$ (this paper) and $d = 4, 5, 6$ (cf. [63]),

For convenience, we will use KST to stand for Kolmogorov superposition theorem for the rest of the paper. Let us start with the statement of KST using the version of G. G. Lorentz from [47] and [48].

Theorem 2 (Kolmogorov Superposition Theorem) *There exist irrational numbers $0 < \lambda_p \leq 1$ for $p = 1, \dots, d$ and strictly increasing Lip(α) functions $\phi_q(x)$ (independent of f) with $\alpha = \log_{10} 2$ defined on $I = [0, 1]$ for $q = 0, \dots, 2d$ such that for every continuous function f defined on $[0, 1]^d$,*

there exists a continuous function $g(u)$, $u \in [0, d]$ such that

$$f(x_1, \dots, x_d) = \sum_{q=0}^{2d} g\left(\sum_{i=1}^d \lambda_i \phi_q(x_i)\right). \quad (2)$$

Note that $\phi_q, q = 0, \dots, 2d$ are called inner functions while g is called outer function. In the original version of KST (cf. [33], [34]), there are $2d + 1$ outer functions and $d(2d + 1)$ inner functions. G. G. Lorentz simplified the construction to have one outer function and $2d + 1$ inner functions with d irrational numbers λ_i . See [50] for KST with one outer function and $d(2d + 1)$ inner functions. It is known that $2d + 1$ can not be smaller (cf. [14]) and the smoothness of the inner functions in the original version of the KST can be improved to be Lipschitz continuous (cf. [20]) while the continuity of ϕ_q in the Lorentz version can be improved to be Lip_α for any $\alpha \in (0, 1)$ as pointed out in [48] at the end of the chapter. There were Sprecher's constructive proofs (cf. [69, 70, 71, 72, 73, 74, 75, 76]) which were finally correctly established in [5] and [6]. An excellent explanation of the history on the KST can be found in [56] together with a constructive proof similar to the Lorentz construction.

Recently, KST has been extended to unbounded domain in [43] and has been actively studied during the development of the neural network computing (cf. e.g. [10], [52], [57], [54]) as well as during the fast growth period of the deep learning computation recently. Hecht-Nielsen [29] is among the first to explain how to use the KST as a feed forward neural network in 1987. In particular, Igel'nik and Parikh [31] in 2003 proposed an algorithm of the neural network using spline functions to approximate both the inner functions and outer function g . More recently, in [44], the researchers have created a new way to implement two layer neural networks inspired by the Kolmogorov superposition theorem, which experimentally has a better performance than the two Multi-Layer Perceptrons (MLPs). See also [19] for another efficient implementation and numerical results.

It is easy to see that the formulation of the KST is similar to the structure of a neural network where the inner and outer functions can be thought as two hidden layers when approximating a continuous function f . However, one of the main obstacles is that the outer function g depends on f and furthermore, g can vary wildly even if f is smooth as explained in [23]. Schmidt-Hieber [60] used a version of KST in [5] and approximated the inner functions by using a neural network of multiple layers to form a deep learning approach for approximating any Hölder continuous functions. Montanelli and Yang in [54] used very deep neural networks to approximate the inner and outer functions to obtain the approximation rate $O(n^{-\frac{1}{\log d}})$ for a function f in the class $K_C([0, 1]^d)$ (see [54] for detail). That is, the curse of dimensionality is lessened. To the best of our knowledge, the approximation bounds in the existing work for general function still suffer the curse of dimensionality unless f has a simple outer function g as explained in this paper, and how to characterize the class of functions which has moderate outer functions remains an open problem. However, in the last section of this paper, we will provide a numerical method to test if a multi-dimensional continuous function is Kolmogorov-Lipschitz continuous.

The development of the neural networks obtains a great speed-up by using the ReLU function instead of a signmoidal activation function. Sonoda and Murata [68] showed that the ReLU is an approximator and established the universal approximation theorem, i.e. Theorem 3 below. Chen in [8] pointed out that the computation of layers in the deep learning algorithm based on ReLU is a linear spline and studied the upper bound on the number of knots needed for computation. Motivated by the work from [8], Hansson and Olsson in [28] continued the study and gave another justification for the two layers of deep learning are a combination of linear spline and used Tensorflow to train a deep learning machine for approximating the well-known Runge function using a few knots. There are several dissertations written on the study of the KST for the neural networks and data/image classification. See [7], [5], [21], [45], and etc..

The main contribution of this work is we propose to study the rate of approximation for ReLU neural network through KST. We propose a special neural network structure via the representation of KST, which can achieve a dimension independent approximation rate $O(1/n)$ with the approximation constant increasing quadratically in the dimension when approximating a dense subset of continuous functions. The number of parameters used in such a network increases linearly in n . Furthermore, we shall provide a numerical scheme to practically approximate d dimensional continuous functions by using at most $O(dn)$ number of pivotal locations for function value evaluation instead of the whole equally-spaced $O(n^d)$ data locations, and such a set of pivotal locations are independent of target functions.

The subsequent sections of this paper are structured as follows. In section 2, we explain how to use KST to approximate multivariate continuous functions without the curse of dimensionality for a certain class of functions. We also establish the approximation result for any continuous function based on the modulus of continuity of the outer function. In section 4, we introduce KB-splines and its smoothed version LKB-splines. We will show that KB-splines are indeed the basis for functions in $C([0, 1]^d)$. In section 5, we numerically demonstrate in 2D and 3D that LKB-splines can approximate functions in $C([0, 1]^d)$ very well. Furthermore, we provide a computational strategy based on matrix cross approximation to find a sparse solution using a few number of LKB-splines to achieve the same approximation order as the original approximation. This leads to the new concept of pivotal point set from any dense point set P over $[0, 1]^d$ such that the discrete least squares (DLS) fitting based on the pivotal point set has the similar rooted mean squares error to the DLS fitting based on the original data set P .

2 Universal Approximation via KST

We will use σ_1 to denote ReLU function through the rest of discussion. It is easy to see that one can use linear splines to approximate the inner (continuous and monotone increasing) functions $\phi_q, q = 0, \dots, 2d$ and outer (continuous) function g . We refer to Theorem 20.2 in [59]. On the other hand, we can easily see that any linear spline function can be written in terms of linear combination of ReLU functions and vice versa, see, e.g. [11], and [13]. (We shall include another proof later in this paper.) Hence, we have

$$L_q(t) := \sum_{j=1}^{N_q} c_{q,j} \sigma_1(t - y_{qj}) \approx \phi_q(t)$$

for $q = 0, \dots, 2d$ and

$$S_g(t) := \sum_{k=1}^{N_g} w_k \sigma_1(t - y_k) \approx g,$$

where g is the outer function of a continuous function f . Based on KST and the universal approximation theorem (cf. [10], [30], [57]), it follows that

Theorem 3 (Universal Approximation Theorem (cf. [68])) *Suppose that $f \in C([0, 1]^d)$ is a continuous function. For any given $\epsilon > 0$, there exist coefficients $w_k, k = 1, \dots, N_g$, $y_k \in [0, d], k = 1, \dots, N_g$, $c_{q,j}, j = 1, \dots, N_i$ and $y_{q,j} \in [0, 1], j = 1, \dots, N_i$ such that*

$$|f(x_1, \dots, x_d) - \sum_{q=0}^{2d} \sum_{k=1}^{N_g} w_k \sigma_1(\sum_{i=1}^d \lambda_i \sum_{j=1}^{N_i} c_{q,j} \sigma_1(x_i - y_{qj}) - y_k)| \leq \epsilon. \quad (3)$$

In fact, many results similar to the above (3) have been established using other activation functions including learnable activation functions (cf. e.g. [10], [35], [54], [44], and etc.). We shall present a rate of convergence in this section. See (10).

2.1 Kolmogorov-Lipschitz (KL) Functions

To establish the rate of convergence for Theorem 3, we introduce a new concept called Kolmogorov-Lipschitz (KL) continuity. For each continuous function $f \in C([0, 1]^d)$, let g_f be the outer function associated with f . We define

$$KL := \{f : \text{the outer function } g_f \text{ is Lipschitz continuous over } [0, d]\} \quad (4)$$

be the class of Kolmogorov-Lipschitz (KL) continuous functions. Note that when f is a constant, its outer function $g = \frac{1}{d+1}f$ is also constant (cf. [7]) and hence, is Lipschitz continuous. That is, the function class KL is not empty. Furthermore, we can use any univariate Lipschitz continuous function g such as $g(t) = Ct$, $g(t) = \sin(Ct)$, $g(t) = \exp(-Ct)$, $g(t) = \sin(Ct^2/2)$, etc.. over $[0, d]$ to define a multivariate function f by using the formula (2) of KST, where C is any constant. Then these newly defined f are continuous over $[0, 1]^d$, and belong to the function class KL with Lipschitz constant C which is independent of the dimensionality d .

On the other hand, we can use $g(t) = t^d$ or $g(t) = t^{d^d}$ or $g(t) = \sin(d^d t \pi)$ over $[0, d]$ to define a multivariate continuous function by the KST formula (2) in $C[0, 1]^d$. These functions either grow exponentially when $d \geq 3$ is large or oscillate very quickly that spoil the fun of constructing an approximation scheme which overcomes the curse of dimensionality. In general, such pathological functions will seldom appear in practice. For practical purposes, we shall restrict some classes of multidimensional functions to avoid these pathological functions. To do so, we let $\bigcup_{d=2}^{\infty} C([0, 1]^d)$ be the algebraic union of these continuous function spaces $C([0, 1]^d)$'s. Note that any function in $C([0, 1]^d)$ can be extended naturally to be a function in $C([0, 1]^{d+1})$ and hence, can be extended to be a continuous function in infinitely many variables. Hence, we define by

$$C([0, 1]^\infty) = \text{closure of } \bigcup_{d=2}^{\infty} C([0, 1]^d) \text{ in the } L^\infty \text{ norm} \quad (5)$$

the Banach space of the maximal norm completion of $\bigcup_{d=2}^{\infty} C([0, 1]^d)$. Furthermore, we say a function $f \in C([0, 1]^\infty)$ is a Kolmogorov-Lipschitz (KL) continuous function with KL constant C if there is a sequence of KL continuous functions f_n in $C([0, 1]^{d_n})$ with KL constant $\leq C$ such that $f_n \rightarrow f$ in the maximal norm. Let $KL([0, 1]^\infty)$ be the class of all Kolmogorov-Lipschitz functions in $C([0, 1]^\infty)$. We shall show that these functions in $KL([0, 1]^\infty)$ will be dense in $C([0, 1]^\infty)$. We shall use this space $C([0, 1]^\infty)$ to explain the curse of dimensionality later in the paper.

It is easy to see that the class KL is dense in $C([0, 1]^d)$ by Weierstrass approximation theorem for any fixed dimensionality $d > 1$. See Theorem 4 below. For another example, let $g(t)$ be a B-spline function of degree $k \geq 1$, the associated multivariate function is in KL. We shall use such B-spline functions for the outer function g approximation in a later section.

Theorem 4 *Fix any integer $d \geq 2$. For any $f \in C([0, 1]^d)$ and any $\epsilon > 0$, there exists a KL continuous function K_ϵ dependent on ϵ such that*

$$\|f - K_\epsilon\|_\infty \leq \epsilon. \quad (6)$$

Furthermore, the Kolmogorov-Lipschitz (KL) constant C of K_ϵ is $C = O(n^2 4^{2n} \|g_f\|_\infty / d)$, where g_f is the outer function of f and n is dependent on ϵ as described in the proof.

Proof. By the KST, we can write $f(x_1, \dots, x_d) = \sum_{q=0}^{2d+1} g(\sum_{i=1}^d \lambda_i \phi_q(x_i))$. By Weierstrass approximation theorem, there exists a polynomial p_ϵ such that $|p_\epsilon(t) - g(t)| \leq \frac{\epsilon}{2d+1}$ for all $t \in [0, d]$. Such a polynomial p_ϵ is certainly a Lipschitz continuous function over $[0, d]$ whose Lipschitz constant will be given soon.

Therefore, by letting $K_\epsilon(x_1, \dots, x_d) = \sum_{q=0}^{2d+1} p_\epsilon(\sum_{i=1}^d \lambda_i \phi_q(x_i)) \in KL$, we have a simple formula

$$\begin{aligned} |f(x_1, \dots, x_d) - K_\epsilon(x_1, \dots, x_d)| &= \left| \sum_{q=0}^{2d+1} g\left(\sum_{i=1}^d \lambda_i \phi_q(x_i)\right) - \sum_{q=0}^{2d+1} p_\epsilon\left(\sum_{i=1}^d \lambda_i \phi_q(x_i)\right) \right| \\ &\leq \sum_{q=0}^{2d+1} \left| g\left(\sum_{i=1}^d \lambda_i \phi_q(x_i)\right) - p_\epsilon\left(\sum_{i=1}^d \lambda_i \phi_q(x_i)\right) \right| \\ &\leq (2d+1) \cdot \frac{\epsilon}{(2d+1)} = \epsilon. \end{aligned}$$

To specify the Lipschitz constant of the polynomial p_ϵ , we recall the well-known Fejér-Hermite polynomials which is defined by

$$F_n(g; x) = \sum_{i=1}^n g(x_i) [1 - 2Dl_i(x_i)(x - x_i)] L_i^2(x) \quad (7)$$

where $L_i(x) = \prod_{\substack{j=1 \\ j \neq i}}^n \frac{(x - x_j)}{(x_i - x_j)}$, $i = 1, \dots, n$ and $\{x_1, \dots, x_n\} \subseteq [a, b]$ is a set of distinct knots. We refer to [9] for detail. Furthermore, for $[a, b] = [-1, 1]$ and the distinct knots chosen to be the zero of Tchebysheff polynomial T_n of degree n , we have

$$F_n(g; x) = \frac{T_n^2(x)}{n^2} \sum_{i=1}^n g(x_i) \frac{1 - xx_i}{(x - x_i)^2},$$

where $x_i = \cos(2i - 1)\pi/2n$, $i = 1, \dots, n$. (See, p. 79 of [9].) When $g \in C[-1, 1]$, since $F_n(1; x) = 1$, for $x \in [-1, 1]$, we have

$$F_n(g; x) - g(x) = \frac{T_n^2(x)}{n^2} \sum_{i=1}^n (g(x_i) - g(x)) \frac{1 - xx_i}{(x - x_i)^2}.$$

$$\begin{aligned} |F_n(g; x) - g(x)| &\leq \frac{T_n^2(x)}{n^2} \left(\sum_{|x-x_i| < \delta} \epsilon \frac{1 - xx_i}{(x - x_i)^2} + \sum_{|x-x_i| \geq \delta} 2\|g\|_\infty \frac{1 - xx_i}{(x - x_i)^2} \right) \\ &\leq \frac{T_n^2(x)}{n^2} \left(\epsilon \sum_{i=1}^n \frac{1 - xx_i}{(x - x_i)} + \frac{2\|g\|_\infty}{\delta^2} \sum_{i=1}^n (x - x_i)^2 \frac{1 - xx_i}{(x - x_i)^2} \right) \\ &= \epsilon + \frac{2\|g\|_\infty}{\delta^2 n^2} \sum_{i=1}^n (1 - xx_i) \leq \epsilon + \frac{4\|g\|_\infty}{\delta^2 n^2} \cdot n \leq 2\epsilon \quad \text{when } n \text{ large enough.} \end{aligned}$$

In fact, n is so large such that $n \geq \sqrt{2\|g\|_\infty/(\delta^2 \epsilon)}$.

Let us convert the polynomial F_n to be over $[0, d]$ with $g = g_f \in C[0, d]$, the above estimate can be carried out as well to establish the convergence. Now let us estimate its Lipschitz constant of F_n .

It is easy to see the Fejér-Hermite polynomial is $F_n(g; -1 + 2x/d)$ over $[0, d]$ and more precisely,

$$F_n(g; -1 + 2x/d) = \frac{T_n^2(-1 + 2x/d)}{n^2} \sum_{i=1}^n g_f(y_i) \frac{2xd + 2dy_i - 4xy_i}{4(x - y_i)^2},$$

where $y_i = d(x_i + 1)/2 \in [0, d]$ for $i = 1, \dots, n$. If we write $F_n(g; -1 + 2x/d) = a_0x^{2n-1} + a_1x^{2n-2} + \dots$, then

$$a_0 = \lim_{x \rightarrow \infty} \frac{F_n(g; -1 + 2x/d)}{x^{2n-1}} = \frac{1}{n^2} \lim_{x \rightarrow \infty} \frac{2^{2n} T_n^2(-1 + 2x/d)}{d^{2n} (2x/d - 1)^{2n}} \sum_{i=1}^n g(y_i) \frac{x(2xd + 2dy_i - 4xy_i)}{4(x - y_i)^2}$$

and hence, $|a_0| \leq 4^{2n}/d^{2n} \|g\|_\infty \sum_{i=1}^n |d/2 - y_i|$ since the leading coefficient of T_n is 2^n . We know that the Lipschitz constant C of $F_n(g; -1 + 2x/d)$ is bounded by $\|F'_n(g; \cdot)\|_\infty \leq (2n-1)(|a_0|d^{2n-2} + |a_1|d^{2n-3} + \dots) = O((2n-1)|a_0|d^{2n-2})$ when $d \gg 2$. It now follows that the Lipschitz constant C of F_n is

$$C \leq \frac{(2n-1)d^{2n-2}4^{2n}}{d^{2n}} \|g\|_\infty nd \leq (2n^2)4^{2n} \|g\|_\infty / d. \quad (8)$$

These finish the proof. \square

We are now ready to establish one of our main results in this paper.

Theorem 5 *The class $KL([0, 1]^\infty)$ is dense in $C([0, 1]^\infty)$.*

Proof. Suppose that $f \in C([0, 1]^\infty)$. For any $\epsilon > 0$, we first find $f_d \in C([0, 1]^d)$ such that $\|f - f_d\|_\infty \leq \epsilon/2$. Since f is bounded, so is f_d . We use Theorem 4 to have a KL polynomial P_ϵ such that

$$\|f_d - P_\epsilon\|_\infty \leq \epsilon/2.$$

It follows that $\|f - P_\epsilon\|_\infty \leq \|f - f_d\|_\infty + \|f_d - P_\epsilon\|_\infty \leq \epsilon$. Note that based on the constructive proof of Kolmogorov superposition theorem, we know K-outer function g_f is bounded and hence, the Kolmogorov-Lipschitz constant C is bounded independent of d based on the estimate in (8). \square

Based on the discussion above, we now focus on the multidimensional functions which are Kolmogorov-Lipschitz continuous functions.

3 Approximation via ReLU Neural Networks

In this section, we study the approximation of multivariate continuous functions by using the standard ReLU neural networks. Note that the neural network being used for approximation in expression (3) is a special class of neural network with two hidden layers of widths $(2d+1)dN_q$ and $(2d+1)N_g$ respectively. Let us call this special class of neural networks the Kolmogorov network, or K-network in short and use $\mathcal{K}_{m,n}$ to denote the K-network of two hidden layers with widths $(2d+1)dm$ and $(2d+1)n$ based on ReLU activation function, i.e.,

$$\mathcal{K}_{m,n}(\sigma_1) = \left\{ \sum_{q=0}^{2d} \sum_{k=1}^{dn} w_k \sigma_1 \left(\sum_{i=1}^d \sum_{j=1}^m c_{qj} \sigma_1(x_i - y_{qj}) - y_k \right), w_k, c_{qj} \in \mathbb{R}, y_k \in [0, d], y_{qj} \in [0, 1] \right\}. \quad (9)$$

The parameters in $\mathcal{K}_{m,n}$ are $w_k, y_k, k = 1, \dots, dn$, and $c_{qj}, y_{qj}, q = 0, \dots, 2d, j = 1, \dots, m$. Therefore the total number of parameters equals to $2dn + 2(2d+1)m$. In particular if $m = n$, the total number of parameters in this network is $(6d+2)n$. We are now ready to state another one of the main results in this paper.

Theorem 6 *Let $f \in C([0, 1]^d)$ and assume f is in the class $KL([0, 1]^\infty)$. Let C_f be the Kolmogorov-Lipschitz constant of f , i.e. the Lipschitz constant of the K -outer function g_f associated with f . We have*

$$\inf_{s \in \mathcal{K}_{n,n}(\sigma_1)} \|f - s\|_{C([0,1]^d)} \leq \frac{C_f(2d+1)^2}{n}. \quad (10)$$

The significance of this result is that we need only $(6d+2)n$ parameters to achieve the approximation rate $O(1/n)$ with the approximation constant increasing quadratically in the dimension if C_f bounded or growing moderately in d . To overcome the curse of dimensionality when approximating f , we shall discuss how to use $O(nd)$ data points and values to achieve the order of the convergence in (10) in the later sections.

To prove Theorem 6, we need some preparations. Let us begin with the space $\mathcal{N}(\sigma_1) = \text{span}\{\sigma_1(\mathbf{w}^\top \mathbf{x} - b), b \in \mathbb{R}, \mathbf{w} \in \mathbb{R}^d\}$ which is the space of shallow networks of ReLU functions. It is easy to see that all linear polynomials over \mathbb{R}^d are in $\mathcal{N}(\sigma_1)$. The following result is known (cf. e.g. [11]). For self-containedness, we include a different proof.

Lemma 1 *For any linear polynomial s over \mathbb{R}^d , there exist coefficients $c_i \in \mathbb{R}$, bias $t_i \in \mathbb{R}$ and weights $\mathbf{w}_i \in \mathbb{R}^d$ such that*

$$s(\mathbf{x}) = \sum_{i=1}^n c_i \sigma_1(\mathbf{w}_i \cdot \mathbf{x} + t_i), \forall \mathbf{x} \in [0, 1]^d. \quad (11)$$

That is, $s \in \mathcal{N}(\sigma_1)$.

Proof. It is easy to see that a linear polynomial x can be exactly reproduced by using the ReLU functions. For example,

$$x = \sigma_1(x), \forall x \in [0, 1]. \quad (12)$$

Hence, any component x_j of $\mathbf{x} \in \mathbb{R}^d$ can be written in terms of (11). Indeed, choosing $\mathbf{w}_i = \mathbf{e}_j$, from (12), we have

$$x_j = \sigma_1(\mathbf{e}_j \cdot \mathbf{x}), \quad \mathbf{x} \in [0, 1]^d, j = 1, \dots, d.$$

Next we claim a constant 1 is in $\mathcal{N}(\sigma_1)$. Indeed, given a partition $\mathcal{P}_n = \{a = x_0 < x_1 < \dots < x_n = b\}$ of interval $[a, b]$, let

$$h_0(x) = \begin{cases} \frac{x - x_1}{x_0 - x_1} & x \in [x_0, x_1] \\ 0 & x \in [x_1, x_n] \end{cases}, \quad (13)$$

$$h_i(x) = \begin{cases} \frac{x - x_{i-1}}{x_i - x_{i-1}} & x \in [x_{i-1}, x_i] \\ \frac{x - x_{i+1}}{x_i - x_{i+1}} & x \in [x_i, x_{i+1}] \\ 0 & x \notin [x_{i-1}, x_{i+1}] \end{cases}, \quad i = 1, \dots, n-1 \quad (14)$$

$$h_n(x) = \begin{cases} \frac{x - x_{n-1}}{x_n - x_{n-1}} & x \in [x_{n-1}, x_n] \\ 0 & x \in [x_0, x_{n-1}] \end{cases}. \quad (15)$$

be a set of piecewise linear spline functions over \mathcal{P}_n . Then we know $S_1^0(\mathcal{P}_n) = \text{span}\{h_i, i = 0, \dots, n\}$ is a linear spline space. It is well-known that $1 = \sum_{i=0}^n h_i(x)$. Now we note the following formula:

$$h_i(x) = \frac{\sigma_1(x - x_{i-1})}{(x_i - x_{i-1})} + w_i \sigma_1(x - x_i) + \frac{\sigma_1(x - x_{i+1})}{(x_{i+1} - x_i)}, \quad (16)$$

where $w_i = -1/(x_i - x_{i-1}) - 1/(x_{i+1} - x_i)$. It follows that any spline function in $S_1^0(\mathcal{P}_n)$ can be written in terms of ReLU functions. In particular, we can write $1 = \sum_{i=0}^n h_i(x) = \sum_{i=0}^n c_i^0 \sigma_1(x - x_i)$ by using (16).

Hence, for any linear polynomial $s(\mathbf{x}) = a + \sum_{j=1}^d c_j x_j$, we have

$$s(\mathbf{x}) = a \sum_{i=0}^n c_i^0 \sigma_1(x - x_i) + \sum_{i=1}^d c_i \sigma_1(\mathbf{e}_i \cdot \mathbf{x}) \in \mathbb{N}(\sigma_1).$$

This completes the proof. \square

The above result shows that any linear spline is in the ReLU neural networks. Also, any ReLU neural network in \mathbb{R}^1 is a linear spline. We are now ready to prove Theorem 6. We begin with the standard modulus of continuity. For any continuous function $g \in C[0, d]$, we define the modulus of continuity of g by

$$\omega(g, h) = \max_{\substack{x \in [0, d] \\ 0 < t \leq h}} |g(x+t) - g(x)| \quad (17)$$

for any $h > 0$. To prove the result in Theorem 6, we need to recall some basic properties of linear splines (cf. [61]). The following result was established in [59].

Lemma 2 *For any function in $f \in C[a, b]$, there exists a linear spline $S_f \in S_1^0(\Delta)$ such that*

$$\|f - S_f\|_{\infty, [a, b]} \leq \omega(f, |\Delta|) \quad (18)$$

where $S_1^0(\Delta)$ is the space of all continuous linear splines over the partition $\Delta = \{a = t_0 < t_1 < \dots < t_n = b\}$ with $|\Delta| = \max_i |t_i - t_{i-1}|$.

In order to know the rate of convergence, we need to introduce the class of function of bounded variation. We say a function f is of bounded variation over $[a, b]$ if

$$\sup_{\forall a=x_0 < x_1 < \dots < x_n=b} \sum_{i=1}^n |f(x_i) - f(x_{i-1})| < \infty$$

We let $V_a^b(f)$ be the value above when f is of bounded variation. The following result is well known (cf. [61])

Lemma 3 *Suppose that f is of bounded variation over $[a, b]$. For any $n \geq 1$, there exists a partition Δ with n knots such that*

$$\text{dist}(f, S_1^0(\Delta))_\infty = \inf_{s \in S_1^0(\Delta)} \|f - s\|_\infty \leq \frac{V_a^b(f)}{n+1}.$$

Let $L = \{f \in C([0, 1]^d) : |f(\mathbf{x}) - f(\mathbf{y})| \leq L_f |\mathbf{x} - \mathbf{y}|, \forall \mathbf{x}, \mathbf{y} \in [0, 1]^d\}$ be the class of Lipschitz continuous functions. We can further establish

Lemma 4 *Suppose that f is Lipschitz continuous over $[a, b]$ with Lipschitz constant L_f . For any $n \geq 1$, there exists a partition Δ with n interior knots such that*

$$\text{dist}(f, S_1^0(\Delta))_\infty \leq \frac{L_f(b-a)}{2(n+1)}.$$

Proof. We use a linear interpolatory spline S_f . Then for $x \in [x_i, x_{i+1}]$,

$$\begin{aligned} f(x) - S_f(x) &= f(x) - f(x_i) \frac{x_{i+1} - x}{x_{i+1} - x_i} - f(x_{i+1}) \frac{x - x_i}{x_{i+1} - x_i} \\ &= \frac{(x_{i+1} - x)(f(x) - f(x_i))}{x_{i+1} - x_i} + \frac{(x - x_i)(f(x) - f(x_{i+1}))}{x_{i+1} - x_i} \\ &\leq L_f \frac{(x - x_i)(x_{i+1} - x)}{x_{i+1} - x_i} + L_f \frac{(x_{i+1} - x)(x - x_i)}{x_{i+1} - x_i} \leq \frac{L_f}{2} (x_{i+1} - x_i). \end{aligned}$$

Hence, $|f(x) - S_f(x)| \leq L_f(b - a)/(2(n + 1))$ if $x_{i+1} - x_i = (b - a)/(n + 1)$. This completes the proof. \square

Furthermore, if f is Lipschitz continuous, so is the linear interpolatory spline S_f . In fact, we have

$$|S_f(x) - S_f(y)| \leq L_f|x - y|. \quad (19)$$

We are now ready to prove one of our main results in this paper.

Proof. [Proof of Theorems 6] Since ϕ_q are univariate increasing functions mapping from $[0, 1]$ to $[0, 1]$, they are bounded variation with $V_0^1(\phi_q) \leq 1$. By Lemma 3, there are linear spline functions L_q such that $|L_q(t) - \phi_q(t)| \leq 1/(n + 1)$ for $q = 0, \dots, 2d$.

For K-outer function g_f associated with f , when g_f is Lipschitz continuous, there is a linear spline S_g with dn distinct interior knots over $[0, d]$ such that

$$\sup_{t \in [0, d]} |g_f(t) - S_g(t)| \leq \frac{dC_g}{2(nd + 1)} \leq \frac{C_g}{2n},$$

where C_g is the Lipschitz constant of g by using Lemma 4. Now we first have

$$|f(\mathbf{x}) - \sum_{q=0}^{2d} S_g(\sum_{i=1}^d \lambda_i \phi_q(x_i))| \leq \sum_{q=0}^{2d} |g(\sum_{i=1}^d \lambda_i \phi_q(x_i)) - S_g(\sum_{i=1}^d \lambda_i \phi_q(x_i))| \leq \frac{(2d + 1)C_g}{2n}.$$

Next since g is Lipschitz continuous, so is S_g . Thus, by (19) and Lemma 3, we have

$$|S_g(\sum_{i=1}^d \lambda_i \phi_q(x_i)) - S_g(\sum_{i=1}^d \lambda_i L_q(x_i))| \leq C_g \sum_{i=1}^d \lambda_i |\phi_q(x_i) - L_q(x_i)| \leq \frac{d \cdot C_g}{(n + 1)}.$$

Let us put the above estimates together to have

$$|f(\mathbf{x}) - \sum_{q=0}^{2d} S_g(\sum_{i=1}^d \lambda_i L_q(x_i))| \leq \frac{(2d + 1)C_g}{2n} + \frac{(2d + 1)dC_g}{(n + 1)} \leq \frac{(2d + 1)^2 C_g}{n}.$$

The conclusion of Theorem 6 follows. \square

3.1 Functions Beyond the KL Class

As K-outer function g may not be Lipschitz continuous, we next consider a class of functions which is of Hölder continuity. Letting $\alpha \in (0, 1]$, we say g is in $C^{0, \alpha}$ if

$$\sup_{x, y \in [0, d]} \frac{|g(x) - g(y)|}{|x - y|^\alpha} \leq L_\alpha(g) < \infty. \quad (20)$$

Using such a continuous function g , we can define a multivariate continuous function f by using the formula in Theorem 2. In addition, we can extend the argument for the proof of Theorem 6 to the setting of Kolmogorov-Hölder continuous functions and present the convergence in terms of Kolmogorov-modulus of smoothness. Let us extend the analysis of the proof of Lemma 4 to have

Lemma 5 *Suppose that g is Hölder continuous over $[0, d]$, say $g \in C^{0,\alpha}$ with $L_\alpha(g)$ for some $\alpha \in (0, 1]$. For any $n \geq 1$, there exists a partition Δ with n interior knots such that*

$$\text{dist}(g, S_1^0(\Delta))_\infty \leq \frac{L_\alpha(g)d^\alpha}{2(n+1)^\alpha}.$$

Similarly, we can define a class of functions which is Kolmogorov-Hölder (KH) continuous in the sense that K -outer function g is Hölder continuity $\alpha \in (0, 1)$. For each univariate g in $C^{0,\alpha}([0, d])$, we define f using the KST formula (2). Then we have a new class of continuous functions which will satisfy (21). The proof is a straightforward generalization of the one for Theorem 6, we leave it to the interested readers.

Theorem 7 *For each continuous function $f \in C([0, 1]^d)$, let g be the K -outer function associated with f . Suppose that $g \in C^{0,\alpha}([0, d])$ for some $\alpha \in (0, 1]$. Then*

$$\inf_{s \in \mathcal{K}_{n,n}(\sigma_1)} \|f - s\|_{C([0,1]^d)} \leq \frac{(2d+1)^2 L_\alpha(g)}{n^\alpha}. \quad (21)$$

Finally, in this section, we study the Kolmogorov-modulus of continuity. For any continuous function $f \in C([0, 1]^d)$, let g_f be the K -outer function of f based on the KST. Then we use $\omega(g_f, h)$ which is called the Kolmogorov-modulus of continuity of f to measure the smoothness of g_f . Due to the uniform continuity of g_f , we have linear spline S_{g_f} over an equally-spaced knot sequence such that

$$|g_f(t) - S_{g_f}(t)| \leq \omega(g_f, h), \quad \forall t \in [0, d] \quad (22)$$

for any $h > 0$, e.g. $h = 1/n$ for a positive integer n . It follows that

$$|g_f(\sum_{i=1}^d \lambda_i \phi_q(x_i)) - S_{g_f}(\sum_{i=1}^d \lambda_i \phi_q(x_i))| \leq \omega(g_f, h), \quad (23)$$

for any $(x_1, \dots, x_d) \in [0, 1]^d$. Since $\phi_q, q = 0, \dots, 2d$ are monotonically increasing, we use Lemma 3 to have linear splines L_q such that $|L_q(t) - \phi_q(t)| \leq h$ since $V_0^1(\phi_q) \leq 1$. We now estimate

$$|S_{g_f}(\sum_{i=1}^d \lambda_i \phi_q(x_i)) - S_{g_f}(\sum_{i=1}^d \lambda_i L_q(x_i))| \quad (24)$$

for $q = 0, \dots, 2d$. Note that

$$|\sum_{i=1}^d \lambda_i \phi_q(x_i) - \sum_{i=1}^d \lambda_i L_q(x_i)| \leq \sum_{i=1}^d |\phi_q(x_i) - L_q(x_i)| \leq dh.$$

The difference of the above two points in $[0, d]$ is separated by at most d subintervals with length h and hence, we will have

$$|S_{g_f}(\sum_{i=1}^d \lambda_i \phi_q(x_i)) - S_{g_f}(\sum_{i=1}^d \lambda_i L_q(x_i))| \leq 2d \cdot \omega(g_f, h) \quad (25)$$

since S_{g_f} is a linear interpolatory spline of g_f . It follows that

$$\begin{aligned}
& |f(x_1, \dots, x_n) - \sum_{q=0}^{2d} S_{g_f}(\sum_{i=1}^d \lambda_i L_q(x_i))| \\
& \leq \sum_{q=0}^{2d} |g_f(\sum_{i=1}^d \lambda_i \phi_q(x_i)) - S_{g_f}(\sum_{i=1}^d \lambda_i \phi_q(x_i))| + \sum_{q=0}^{2d} |S_{g_f}(\sum_{i=1}^d \lambda_i \phi_q(x_i)) - S_{g_f}(\sum_{i=1}^d \lambda_i L_q(x_i))| \\
& \leq (2d+1)\omega(g_f, h) + (2d+1)2d \cdot \omega(g_f, h).
\end{aligned}$$

Therefore, we conclude the following theorem.

Theorem 8 *For any continuous function $f \in C[0, 1]^d$, let g_f be the K -outer function associated with f . Then*

$$\inf_{s \in \mathcal{K}_{n,n}(\sigma_1)} \|f - s\|_{C([0,1]^d)} \leq (2d+1)^2 \omega(g_f, 1/n). \quad (26)$$

4 KB-splines and LKB-splines

However, it is not easy to see if the K -outer function g_f is Lipschitz continuous when given a continuous functions f . To do so we have to compute g_f from f first. To this end, we implemented Lorentz's constructive proof of KST in MATLAB by following the steps in pages 168 – 174 in [48]. See [7] for another implementation based on Maple and MATLAB. We noticed that the curve g_f behaviors very badly for many smooth functions f . Even if f is a linear polynomial in the 2-dimensional space, the K -outer function g still behaviors very widely although we can use K -network with two hidden layers to approximate this linear polynomial f arbitrarily well in theory. This may be a big hurdle to prevent researchers in [23], [29], [35], [31], [7], and etc. from successful applications based on Kolmogorov spline network. We circumvent the difficulty of having such a wildly behaved K -outer function g by introducing KB-splines and the denoised counterpart LKB-splines in this section. In addition, we will explain how to use them to well approximate high dimensional functions in a later section.

First of all, we note that the implementation of these $\phi_q, q = 0, \dots, 2d$ is not easy. Numerical ϕ_q 's are not accurate enough. Indeed, letting $z_q(x_1, \dots, x_d) = \sum_{i=1}^d \lambda_i \phi_q(x_i)$, Consider the transform:

$$T(x_1, \dots, x_d) = (z_0, z_1, \dots, z_{2d}) \quad (27)$$

which maps from $[0, 1]^d$ to \mathbb{R}^{2d+1} . Let $Z = \{T(x_1, \dots, x_d), (x_1, \dots, x_d) \in [0, 1]^d\}$ be the image of $T([0, 1]^d) \subset \mathbb{R}^{2d+1}$. It is easy to see that the image is closed. The theory in [48] explains that the map T is one-to-one and continuous. As the dimension of Z is much larger than d , the map T is like a well-known Peano curve which maps from $[0, 1]$ to $[0, 1]^2$ and hence, the implementation of T , i.e., the implementation of ϕ_q 's is not possible to be accurate. However, we are able to compute these ϕ_q and decompose g such that the reconstruction of constant function is exact. Let us present two examples to show that our numerical implementation is reasonable. For convenience, let us use images as 2D functions and compute their K -outer functions g and then reconstruct the images back. In Figure 1, we can see that the reconstruction is very good visually although K -outer functions g are oscillating very much. It is worthwhile to note that such reconstruction results have also been reported in [7]. Certainly, these images are not continuous functions and hence we do not expect that g to be Lipschitz continuous. But these reconstructed images serves as a “proof” that our computational code works numerically.

Next we present a few examples of smooth functions whose K -outer functions may not be Lipschitz continuous in Figure 2. Note that the reconstructed functions are very noisy, in fact they are too noisy

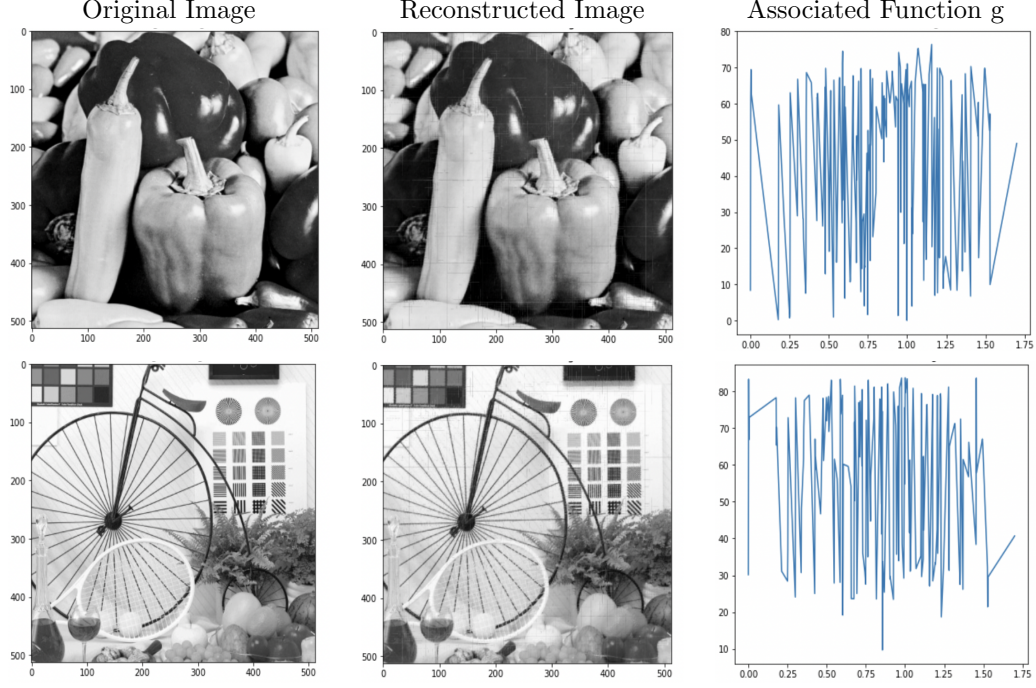


Figure 1: Original image (left column), reconstructed image (middle column), and associated K-outer function g (right column)

to believe that the implementation of the KST can be useful. In order to see that these noisy functions are indeed the original functions, we applied a penalized least squares method based on bivariate spline method (to be explained later in the paper). That is, after denoising, the reconstructed functions are very close to the exact original functions as shown in Figure 2. That is, the denoising method is successful which motivates us to adopt this approach to approximate any continuous functions.

4.1 KB-splines

To this end, we first use standard uniform B-splines to form some subclasses of KL continuous functions. Let $\Delta_n = \{0 = t_1 < t_2 < \dots < t_{dn} < d\}$ be a uniform partition of interval $[0, d]$ and let $b_{n,i}(t) = B_k(t - t_i), i = 1, \dots, dn$ be the standard B-splines of degree k with $k \geq 1$. For simplicity, we only explain our approach based on linear B-splines for the theoretical aspect while using other B-splines (e.g. cubic B-splines) for the numerical experiments. We define KB-splines by

$$KB_{n,j}(x_1, \dots, x_d) = \sum_{q=0}^{2d} b_{n,j} \left(\sum_{i=1}^d \lambda_i \phi_q(x_i) \right), j = 1, \dots, dn. \quad (28)$$

It is easy to see that each of these KB-splines defined above is nonnegative. Due to the property of B-splines: $\sum_{i=1}^{dn} b_{n,i}(t) = 1$ for all $t \in [0, d]$, we have the following property of KB-splines:

Theorem 9 *We have $\sum_{i=1}^{dn} KB_{n,i}(x_1, \dots, x_d) = 1$ and hence, $0 \leq KB_{n,i} \leq 1$.*

Proof. The proof is immediate by using the fact $\sum_{i=1}^{dn} b_{n,i}(t) = 1$ for all $t \in [0, d]$. \square

Remark 1 *The property in Theorem 9 is called the partition of unit which makes the computation stable. We note that a few of these dn KB-splines will be zero since $0 < \lambda_i \leq 1$ and $\min\{\lambda_i, i = 1, \dots, d\} < 1$. The number of zero KB-splines is dependent on the choice of $\lambda_i, i = 1, \dots, d$.*

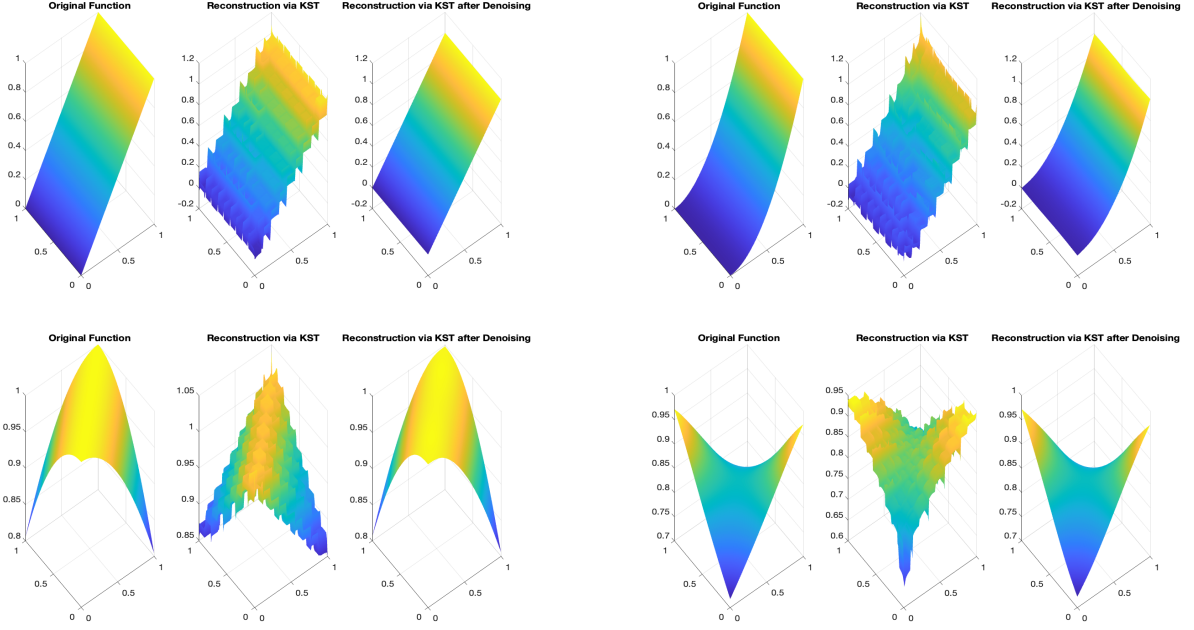


Figure 2: Top left: reconstruction of $f(x, y) = x$. Top right: reconstruction of $f(x, y) = x^2$. Bottom left: reconstruction of $f(x, y) = \cos(2(x - y)/\pi)$. Bottom right: reconstruction of $f(x, y) = \sin(1/(1 + (x - 0.5)(y - 0.5)))$.

Another important result is that these KB-splines are linearly independent.

Theorem 10 *The nonzero KB-splines $\{KB_{n,j} \neq 0, j = 1, \dots, dn\}$ are linearly independent.*

Proof. Suppose there are c_j , $j = 1, 2, \dots, dn$ such that $\sum_{j=1}^{dn} c_j KB_{n,j}(x_1, \dots, x_d) = 0$ for all $(x_1, \dots, x_d) \in [0, 1]^d$. Then we want to show $c_j = 0$ for all $j = 1, 2, \dots, dn$. Let us focus on the case $d = 2$ as the proof for general case d is similar. Suppose $n > 0$ is a fixed integer and we use the notation $z_q = \sum_{i=1}^2 \lambda_i \phi_q(x_i)$ as above. Then based on the graphs of ϕ_q in Figure 3, we can choose $x_1 = \delta$ and $x_2 = 0$ with $0 < \delta \leq 1$ small enough such that $KB_{n,j}(x_1, 0) = \sum_{q=0}^4 b_j(z_q(\delta, 0)) = 0$ for all $j = 3, 4, \dots, 2n$. Therefore in order to show the linear independence of $KB_{n,j}$, $j = 1, 2, \dots, 2n$, it is suffices to show $\sum_{j=1}^2 c_j KB_{n,j}(x_1, x_2) = 0$ implies $c_1 = c_2 = 0$. Let us confine $x_1 \in [0, \delta]$ and $x_2 = 0$. Then we have

$$\begin{aligned} 0 &= c_1 KB_{n,1}(x_1, x_2) + c_2 KB_{n,2}(x_1, x_2) = c_1 \left(\sum_{q=0}^4 b_1(z_q) \right) + c_2 \left(\sum_{q=0}^4 b_2(z_q) \right) \\ &= c_1 \left(\sum_{q=0}^4 b_1(z_q) \right) + c_2 \left(5 - \sum_{q=0}^4 b_1(z_q) \right) = (c_1 - c_2) \left(\sum_{q=0}^4 b_1(z_q) \right) + 5c_2, \end{aligned}$$

where we have used the fact that $b_1(x) + b_2(x) = 1$ over $[0, 1/n]$. Since c_2 is constant, and $\sum_{q=0}^4 b_1(z_q)$ is not constant when x_1 varies between 0 and δ , we must have $c_1 = c_2$. Hence $c_2 = 0$ and therefore $c_1 = 0$.

In the same fashion, we can choose \tilde{x}_1 and $\tilde{\delta}$ such that $KB_{n,j} = \sum_{q=0}^4 b_j(z_q(\tilde{x}_1, 0)) = 0$ for all $j = 1, 2, \dots, 2n$ except for $j = k, k + 1$. By the similar argument as above, we have $c_k = c_{k+1} = 0$. By varying k between 1 and $2n$, we get $c_j = 0$ for all $j = 1, 2, \dots, n$. \square

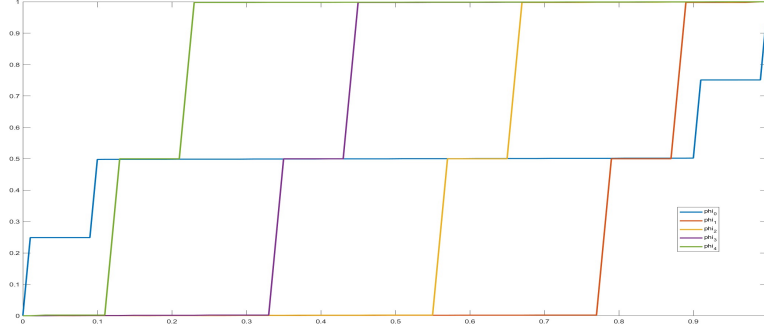


Figure 3: ϕ_q , $q = 0, 1, 2, 3, 4$, in the 2D setting.

Since $\text{span}\{b_{n,i}, i = 1, \dots, nd\}$ will be dense in $C[0, d]$ when $n \rightarrow \infty$, we can conclude that $\text{span}\{KB_{n,j}, j = 1, \dots, nd\}$ will be dense in $C([0, 1]^d)$. That is, we have

Theorem 11 *The KB-splines $KB_{n,j}(x_1, \dots, x_d), j = 1, \dots, nd$ are dense in $C([0, 1]^d)$ when $n \rightarrow \infty$ for a fixed dimension $d \geq 2$.*

Proof. For any continuous function $f \in C([0, 1]^d)$, let $g_f \in C[0, d]$ be the K-outer function of f . For any $\epsilon > 0$, there is an integer $n > 0$ and a spline $S_{g_f} \in \text{span}\{b_{n,i}, i = 1, \dots, dn\}$ such that

$$\|g_f(t) - S_{g_f}(t)\|_\infty \leq \epsilon/(2d + 1) \quad (29)$$

for all t . Note that one can find S_{g_f} by partitioning the interval $[\min(g_f), \max(g_f)]$ into subintervals with length $\epsilon/(2d + 1)$ and find the knots over $[0, d]$ and then add more knots in addition to modify the existing one to obtain a uniform knot sequence. Then S_{g_f} is a linear interpolatory spline of g_f based on the uniform knot sequence.

Writing $S_{g_f}(t) = \sum_{i=1}^{dn} c_i(f)b_{n,i}(t)$, we have

$$\begin{aligned} & |f(x_1, \dots, x_d) - \sum_{i=1}^{dn} c_i(f)KB_{n,i}(x_1, \dots, x_d)| \\ &= \left| \sum_{q=0}^{2d} g(z_q(x_1, \dots, x_d)) - \sum_{i=1}^{dn} c_i(f) \sum_{q=0}^{2d} b_{n,i}(z_q(x_1, \dots, x_d)) \right| \\ &\leq \sum_{q=0}^{2d} |g(z_q(x_1, \dots, x_d)) - S_{g_f}(z_q(x_1, \dots, x_d))| \leq (2d + 1)\epsilon/(2d + 1) = \epsilon. \end{aligned}$$

This completes the proof. \square

Corollary 1 *Suppose that $f \in C([0, 1]^d)$ is Kolmogorov-Lipschitz continuous, that is, the K-outer function $g_f \in C[0, d]$ is Lipschitz with Lipschitz constant L . Then there exists a KB spline $S_n \in \text{span}\{KB_{n,j}(x_1, \dots, x_d), j = 1, \dots, nd\}$ such that*

$$|f(x_1, \dots, x_d) - \sum_{i=1}^{dn} c_i(f)KB_{n,i}(x_1, \dots, x_d)| \leq (2 + 1/d)L/n. \quad (30)$$

Proof. In the proof of Theorem 11, we used the key estimate (29). When g_f is Lipschitz, we have (cf. Theorem 20.2 in [59])

$$\|g_f(t) - S_{g_f}(t)\|_\infty \leq \omega(g_f, 1/(nd)) \leq L/(nd). \quad (31)$$

The rest of the proof is the same as the one in the proof of Theorem 11. \square

Note that the computation of $c_i(f)$'s is not easy as we do not know g_f . We shall explain a computational method to approximate f in the following sections.

4.2 LKB-splines

However, in practice, the KB-splines obtained in (28) are very noisy due to any implementation of ϕ_q 's as we have explained before that the functions $z_q, q = 0, \dots, 2d$, like Peano's curve. One has no way to have an accurate implementation. Also, as demonstrated before, our denoising method can help. We shall call LKB-splines after denoising KB-splines.

Let us explain a multivariate spline method for denoising for $d = 2$ and $d = 3$. In general, we can use tensor product B-splines for denoising for any $d \geq 2$ which is similar to what we are going to explain below. For convenience, let us consider $d = 2$ and let Δ be a triangulation of $[0, 1]^2$ based on a uniform refinement of two triangles by adding a diagonal to $[0, 1]^2$. For any degree $D \geq 1$ and smoothness $r \geq 1$ with $r < D$, let

$$S_D^r(\Delta) = \{s \in C^r([0, 1]^2) : s|_T \in \mathbb{P}_D, T \in \Delta\} \quad (32)$$

be the spline space of degree D and smoothness r with $D > r$. We refer to [38] for a theoretical detail and [2], [62] for a computational detail. For a given data set $\{(x_i, y_i, z_i), i = 1, \dots, N\}$ with $(x_i, y_i) \in [0, 1]^2$ and $z_i = f(x_i, y_i) + \epsilon_i, i = 1, \dots, N$ with noises ϵ_i which may not be very small, the penalized least squares method (cf. [36] and [39]) is to find

$$\min_{s \in S_5^1(\Delta)} \sum_{i=1, \dots, N} |s(x_i, y_i) - z_i|^2 + \lambda \mathcal{E}_2(s) \quad (33)$$

with $\lambda \approx 1$, where $\mathcal{E}_2(s)$ is the thin-plate energy functional defined as follows.

$$\mathcal{E}_2(s) = \int_{\Omega} \left| \frac{\partial^2}{\partial x^2} s \right|^2 + 2 \left| \frac{\partial^2}{\partial x \partial y} s \right|^2 + \left| \frac{\partial^2}{\partial y^2} s \right|^2. \quad (34)$$

Bivariate splines have been studied for several decades and they have been used for data fitting (cf. [36], [39], and [40], [62], and [78]), numerical solution of partial differential equations (see, e.g. [37]), [62], and data denoising (see, e.g. [40]). In our computation, the triangulation Δ is the one obtained from uniformly refined the initial triangulation Δ_0 three times, where Δ_0 is obtained by dividing $[0, 1]^2$ into two triangles using its diagonal line. Let us write $S_5^1(\Delta) = \text{span}\{\phi_1, \dots, \phi_M\}$. For each $k = 1, \dots, dn$, we write $LKB_k = \sum_{j=1}^M c_{k,j} \phi_j$ with coefficients $c_{k,j}$'s being the solution of the linear system:

$$\left(\left[\sum_{i=1}^N \phi_\ell(x_i, y_i) \phi_j(x_i, y_i) \right]_{\ell, j=1, \dots, M} + \lambda E(\phi_\ell, \phi_j) \right) [c_{k,j}] = \left[\sum_{i=1}^N K B_k(x_i, y_i) \phi_\ell(x_i, y_i) \right] \quad (35)$$

for $k = 1, \dots, nd$, where $E(\phi_\ell, \phi_j)$ is the matrix associated with energy functional \mathcal{E}_2 . For convenience, we call the matrix on the left-hand side by A with $\lambda = 1$ fixed.

We now explain that the penalized least squares method can produce a good smooth approximation of the given data. For convenience, let $S_{f,\epsilon}$ be the minimizer of (33) and write $\|f\|_{\mathcal{P}} = \sqrt{\frac{1}{N} \sum_{i=1}^N |f(x_i, y_i)|^2}$ is the rooted mean squares (RMS) which is a semi-norm which is used to measure the computational error. If $f \in C^2([0, 1]^2)$, we have the following

Theorem 12 Suppose that f is twice differentiable over $[0, 1]^2$. Let $S_{f,\epsilon}$ be the minimizer of (33). Then we have

$$\|f - S_{f,\epsilon}\|_{\mathcal{P}} \leq C\|f\|_{2,\infty}|\Delta|^2 + 2\|\epsilon\|_{\mathcal{P}} + \sqrt{\frac{\lambda}{N}}\sqrt{\mathcal{E}_2(f)} \quad (36)$$

for a positive constant C independent of f , degree d , and triangulation Δ .

To prove the above result, let us recall the following minimal energy spline $S_f \in S_5^1(\Delta)$ of data function f : letting Δ be a triangulation of $[0, 1]^2$ with vertices $(x_i, y_i), i = 1, \dots, N$, S_f is the solution of the following minimization:

$$\min_{S_f \in S_5^1(\Delta)} \mathcal{E}_2(S_f) : \quad S_f(x_i, y_i) = f(x_i, y_i), i = 1, \dots, N. \quad (37)$$

Then it is known that S_f approximates f very well if $f \in C^2([0, 1]^2)$. We have

Theorem 13 (von Golitschek, Lai and Schumaker, 2002([77])) Suppose that $f \in C^2([0, 1]^2)$. Then for the minimal energy spline S_f^* which is the solution of (37),

$$\|S_f^* - f\|_{\infty} \leq C\|f\|_{2,\infty}|\Delta|^2 \quad (38)$$

for a positive constant C independent of f and Δ , where $\|f\|_{2,\infty}$ denotes the maximum norm of the second order derivatives of f over $[0, 1]^2$ and $\|S_f^* - f\|_{\infty}$ is the maximum norm of $S_f^* - f$ over $[0, 1]^2$.

Proof.[of Theorem 12] Recall that $S_{f,\epsilon}$ is the minimizer of (33). We now use S_f to have

$$\begin{aligned} \|f - S_{f,\epsilon}\|_{\mathcal{P}} &\leq \|z - S_{f,\epsilon}\|_{\mathcal{P}} + \|\epsilon\|_{\mathcal{P}} \leq \sqrt{\|z - S_{f,\epsilon}\|_{\mathcal{P}}^2 + \frac{\lambda}{N}\mathcal{E}_2(S_{f,\epsilon})} + \|\epsilon\|_{\mathcal{P}} \\ &\leq \frac{1}{\sqrt{N}}\sqrt{\sum_{i=1}^N (z_i - S_f^*(x_i, y_i))^2 + \lambda\mathcal{E}_2(S_f^*)} + \|\epsilon\|_{\mathcal{P}} \\ &\leq \|f - S_f^*\|_{\mathcal{P}} + \|\epsilon\|_{\mathcal{P}} + \sqrt{\frac{\lambda}{N}\mathcal{E}_2(f)} + \|\epsilon\|_{\mathcal{P}} \\ &\leq C\|f\|_{2,\infty}|\Delta|^2 + 2\|\epsilon\|_{\mathcal{P}} + \sqrt{\frac{\lambda}{N}}\sqrt{\mathcal{E}_2(f)}, \end{aligned}$$

where we have used the fact $S_{f,\epsilon}$ is the minimizer of (33) and the fact that $\mathcal{E}_2(S_f^*) \leq \mathcal{E}_2(f)$ which can be found in [77] as well as the estimate in (38). These complete the theorem of this section. \square

Note that the constant C is dependent on the smallest angle of the triangulation Δ . As the domain of interest is $[0, 1]^2$ we use a uniform refinement of the triangulation of two triangles. For $d \geq 3$, we shall use a Delaunay triangulation. So the constant C is not very large. If f is C^2 smooth, then $S_{f,\epsilon}$ will be a good approximation of f when the size $|\Delta|$ of triangulation is small, the thin plate energy $\mathcal{E}_2(f)$ with $\lambda > 0$ is bounded, and the noises $\|\epsilon\|_{\mathcal{P}}$ is small even though a few individual noises ϵ_i can be large. Note also that ϵ can be made small by increasing the accuracy of the implementation of ϕ_q . We also note that the proof of Theorem 13 can be straightforwardly extended to the multi-dimensional setting as soon as the degree D of spline space is large enough.

Now let us illustrate some examples of KB-splines and LKB-splines in Figure 4. One can see that the KB-splines are continuous but not smooth functions at all, while the LKB-splines are very smooth. With these LKB-splines in hand, we can approximate high dimensional continuous functions accurately. Let us report our numerical results in the next section.

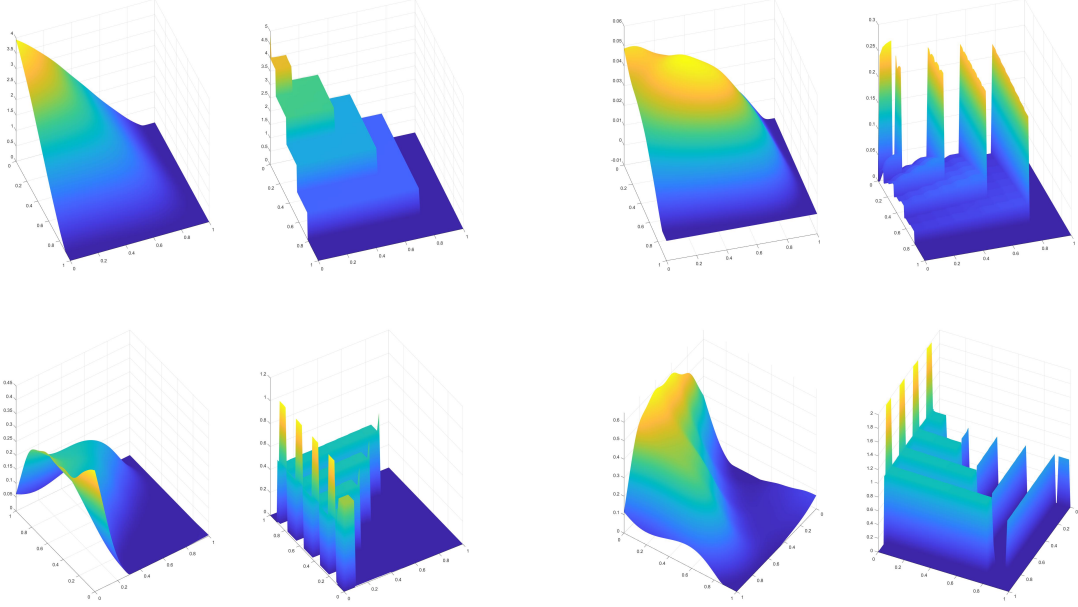


Figure 4: Examples of LKB-splines (first and third columns) which are the smoothed version of the corresponding KB-splines (second and fourth columns).

5 Numerical Approximation by LKB-splines

In this section, we will first show that the LKB-splines are dense in $C([0, 1]^d)$. Then we demonstrate numerically that LKB-splines can approximate general continuous functions well based on $O(n^d)$ equally-spaced sampled data locations. Further, we use the matrix cross approximation technique to show that there are at most $O(nd)$ locations among those $O(n^d)$ locations are pivotal. Therefore, we only need the function values at those pivotal locations in order to achieve a reasonable good approximation.

5.1 The LKB-splines are Dense in $C([0, 1]^d)$

We shall use discrete least squares method to approximate any continuous function f over $[0, 1]^d$. Let $\mathbf{x}_i, i = 1, \dots, N$ be a set of discrete points over $[0, 1]^d$. For example we may use $N = 101^d$ equally-spaced points over $[0, 1]^d$. For any continuous function $f \in C([0, 1]^d)$, we use the function values at these data locations to find an approximation $F_n = \sum_{j=1}^{dn} c_j^* LKB_{n,j}$ by the discrete least squares method which is the solution of the following minimization

$$\min_{c_j} \|f - \sum_{j=1}^{dn} c_j LKB_{n,j}\|_{\mathcal{P}}, \quad (39)$$

where $\|f\|_{\mathcal{P}}$ is the RMS semi-norm based on the function values f over these $N = 101^d$ sampled data points in $[0, 1]^d$. We shall report the accuracy $\|f - F_n(f)\|_{\mathcal{PP}}$, where $\|f\|_{\mathcal{PP}}$ is the RMS semi-norm based on 401^d function values. Recall from Theorem 11 and let $c_j(f)$ be the coefficients of the

KB-spline approximation of f . It is easy to see that

$$\|f - F_n\|_{\mathcal{P}} \leq \|f - \sum_{j=1}^{dn} c_k(f) LKB_{n,k}\|_{\mathcal{P}}. \quad (40)$$

Writing $LKB_{n,k} = \sum_{j=1}^M c_{k,j} \phi_j$ as in the previous section with the coefficient vector

$$[c_{k,j}] = A^{-1} \left[\sum_{i=1}^N KB_k(x_i, y_i) \phi_j(x_i, y_i) \right],$$

where A is the matrix as in (35), we see that

$$\begin{aligned} \sum_{k=1}^{dn} c_k(f) LKB_{n,k} &= \sum_{k=1}^{dn} c_k(f) \sum_{j=1}^M c_{k,j} \phi_j \\ &= \sum_{k=1}^{dn} c_k(f) \sum_{j=1}^M A^{-1} \left[\sum_{i=1}^N KB_{n,k}(x_i, y_i) \phi_j(x_i, y_i) \right] \phi_j \\ &= \sum_{j=1}^M A^{-1} \left[\sum_{i=1}^N \sum_{k=1}^{dn} c_k(f) KB_{n,k}(x_i, y_i) \phi_j(x_i, y_i) \right] \phi_j \\ &= \sum_{j=1}^M A^{-1} \left[\sum_{i=1}^N (f(x_i, y_i) + O(\epsilon)) \phi_j(x_i, y_i) \right] \phi_j, \end{aligned}$$

where we have used the proof of Theorem 11. i.e. $\sum_{k=1}^{dn} c_k(f) KB_{n,k}(x_i, y_i) = f(x_i, y_i) + O(\epsilon)$. Now we note that the right-hand side of the equations above is simply $S_{f,\epsilon}$. That is,

$$\sum_{j=1}^{dn} c_k(f) LKB_{n,k} = S_{f,\epsilon}. \quad (41)$$

By Theorem 12, we conclude the following

Theorem 14 *Suppose that f is twice differentiable over $[0, 1]^2$. Let F_n be the discrete least squares approximation of f defined in (39). Suppose that the points $\mathbf{x}_i = (x_i, y_i)$ for (39) are the same as the points for denoising KB-splines to have the LKB functions. Then*

$$\|f - F_n\|_{\mathcal{P}} \leq C \|f\|_{2,\infty} |\Delta|^2 + 2\|\epsilon\|_{\mathcal{P}} + \frac{1}{\sqrt{N}} \sqrt{\mathcal{E}_2(f)} \quad (42)$$

for a positive constant C independent of f and triangulation Δ .

Although our discussion above is based on the case $d = 2$, all the proofs can be extended to the dimensionality $d > 2$. We next explain that the computation of discrete least squares (39) can be done based on much simpler data points and function values in the following subsection.

5.2 The pivotal data locations for breaking the curse of dimensionality

For convenience, let us use M to indicate the data matrix associated with the discrete least squares problem (39). In other words, for $1 \leq j \leq dn$, the j th column $M(:, j)$ consists of $\{LK B_{n,j}(\mathbf{x}_i)\}$ where $\mathbf{x}_i \in [0, 1]^d$ are those 41^d equally-spaced sampled points in 2D or 3D. Clearly, the experiment above requires 41^d data values which suffers from the curse of dimensionality. However, we in fact do not need such many data values. The main reason is that the data matrix M has many zero columns or near zero columns due to the fact that for many $i = 1, \dots, nd$, the locations from 41^d equally-spaced points do not fall into the support of linear B-splines $b_{n,i}(t)$, $t \in [0, d]$, based on the map z_q . The structures of M are shown in Figure 5 for the case of $n = 1000$ when $d = 2$.

That is, there are many columns in M whose entries are zero or near zero. Therefore, there exists a sparse solution to the discrete least squares fitting problem. We adopt the well-known orthogonal matching pursuit (OMP) (cf. e.g. [42]) to find a solution. For convenience, let us explain the sparse solution technique as follows. Over those 41^d points $\mathbf{x}_i \in [0, 1]^d$, the columns in the matrix

$$M = [LK B_{n,j}(\mathbf{x}_i)]_{i=1, \dots, 41^d, j=1, \dots, dn} \quad (43)$$

are not linearly independent. Let Φ be the normalized matrix of M in (43) and $\mathbf{b} = [f(\mathbf{x}_i)]_{i=1, \dots, 41^d}$. Write $\mathbf{c} = (c_1, \dots, c_{dn})^\top$, we look for

$$\min \|\mathbf{c}\|_0 : \Phi \mathbf{c} = \mathbf{b} \quad (44)$$

where $\|\mathbf{c}\|_0$ stands for the number of nonzero entries of \mathbf{c} . See many numerical methods in ([42]). The near zero columns in Φ also tell us that the data matrix associated with (39) of size $41^d \times dn$ is not full rank $r < dn$. The LKB-splines associated with these near zero columns do not play a role. Therefore, we do not need all dn LKB-splines. Furthermore, let us continue to explain that many data locations among these 41^d locations do not play an essential role.

To this end, we use the so-called matrix cross approximation (see [25], [26], [53], [22], [27], [1] and the literature therein). Let $r \geq 1$ be a rank of the approximation. It is known (cf. [25]) that when $M_{I,J}$ of size $r \times r$ has the maximal volume among all submatrices of M of size $r \times r$, we have

$$\|M - M_{:,J} M_{I,J}^{-1} M_{I,:}\|_C \leq (1 + r) \sigma_{r+1}(M), \quad (45)$$

where $\|\cdot\|_C$ is the Chebyshev norm of matrix and $\sigma_{r+1}(M)$ is the $r + 1$ singular value of M , $M_{I,:}$ is the row block of M associated with the indices in I and $M_{:,J}$ is the column block of M associated with the indices in J . The volume of a square matrix A is the absolute value of the determinant of A .

Note that the estimate in (45) is not very good as when $\sigma_k(M) = O(1/k)$, there is no approximation at all. The estimate is recently improved in [1] which is given in (49).

We mainly find a submatrix $M_{I,J}$ of M such that $M_{I,J}$ has the maximal volume among all $r \times r$ submatrices of M . In practice, we use the concept called dominant matrix to replace the maximal volume and then there are several algorithms, e.g. maxvol algorithm, available in the literature. We use a few greedy based maximal volume search algorithms developed in [1]. These greedy based maxvol algorithms enable us to find a good submatrix $M_{I,J}$ which leads to solve a much simpler discrete least squares problem

$$[M_{I,J} M_{I,J^c}] \hat{\mathbf{x}} = \mathbf{f}_I \quad (46)$$

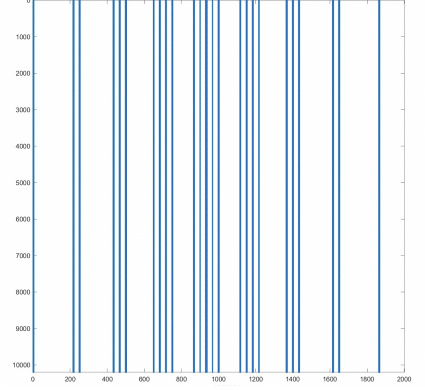


Figure 5: The sparsity pattern of data matrix for $n = 1000$.

where $\mathbf{f} = [\mathbf{f}_I; \mathbf{f}_{I^c}]$ and

$$M = \begin{bmatrix} M_{I,J} & M_{I,J^c} \\ M_{I^c,J} & M_{I^c,J^c} \end{bmatrix}. \quad (47)$$

according to [1] or simply

$$M_{I,J} \hat{\mathbf{x}} = \mathbf{f}_I, \quad (48)$$

as $M_{I^c,J^c} \approx 0$ according to our X_{data} above. We use the same analysis in [1] to have

$$\|M_{I^c,J^c} - M_{I^c,J} M_{I,J}^{-1} M_{I,J^c}\|_C \leq \frac{(r+1)\sigma_{r+1}(M)}{\sqrt{1 + \sum_{k=1}^r \frac{\sigma_{r+1}^2(M)}{\sigma_k^2(M)}}}. \quad (49)$$

In fact, we choose the rank r of M so that the above term is zero. Furthermore, letting $\delta = M\mathbf{x} - \mathbf{f}$ be the residual vector of the discrete least squares approximation (39), we write $\delta = [\delta_I; \delta_{I^c}]$. Then the detail calculation in [1] shows that

$$\begin{aligned} M_{I^c,J} \hat{\mathbf{x}} - \mathbf{f}_{I^c} &= M_{I^c,J} M_{I,J}^{-1} \mathbf{f}_I - \mathbf{f}_{I^c} \\ &= M_{I^c,J} M_{I,J}^{-1} \delta_I + \begin{bmatrix} 0_{I^c,J} & M_{I^c,J} M_{I,J}^{-1} M_{I,J^c} - M_{I^c,J^c} \end{bmatrix} \mathbf{x}_b + \delta_{I^c} \\ &= M_{I^c,J} M_{I,J}^{-1} \delta_I + \delta_{I^c} \end{aligned}$$

since the middle term on the right-hand side is zero as explained above. For simplicity, the solution $\hat{\mathbf{x}}$ of (48) with size $r \times 1$ is also viewed as a vector in the original size $nd \times 1$ with zeros over the index set I^c . Then the root mean square error

$$\|M\hat{\mathbf{x}} - \mathbf{f}\|_{\mathcal{P}} = \|M_{I^c,J} \hat{\mathbf{x}} - \mathbf{f}_{I^c}\|_{\mathcal{P}} \leq \|M_{I^c,J} M_{I,J}^{-1} \delta_I\|_{\mathcal{P}} + \|\delta_{I^c}\|_{\mathcal{P}}.$$

The first term on the right-hand side can be estimated as follows. By the property of $M_{I,J}$, we know that all the entries of $M_{I^c,J} M_{I,J}^{-1}$ are less than or equal to 1. So the ℓ_2 norm $\|M_{I^c,J} M_{I,J}^{-1} \delta_I\|_2 \leq \sqrt{r} \|\delta_I\|_2^2$ and hence,

$$\|M_{I^c,J} M_{I,J}^{-1} \delta_I\|_{\mathcal{P}} \leq \sqrt{r/N} \|\delta_I\|_2.$$

Hence, the solution $\hat{\mathbf{x}}$ in (48) is a good approximation of \mathbf{x}_f , the least squares solution vector (39). More precisely, we have

Theorem 15 ([1]) *Let the residual vector $\delta = M\mathbf{x}_f - \mathbf{f}$ and write $\delta = [\delta_I; \delta_{I^c}]$. Then we have*

$$\|M\hat{\mathbf{x}} - \mathbf{f}\|_{\mathcal{P}} \leq \sqrt{r/N} \|\delta_I\|_2 + \|\delta_{I^c}\|_{\mathcal{P}}. \quad (50)$$

Let \hat{F}_n be the associated LKB spline approximation of f , i.e. $\hat{F}_n = [LKB_{n,1}, \dots, LKB_{n,nd}] \hat{\mathbf{x}}$. We now show that $\hat{F}_n \approx f$. First, recall Theorem 14, for a continuous function $f \in C^2([0, 1]^2)$, the solution F_n of the discrete least squares approximation (39) approximates f very well. That is, the RMS error $\|f - F_n\|_{\mathcal{P}} = \|\delta\|_{\mathcal{P}}$ with

$$\|\delta\|_{\mathcal{P}} \leq C \|f\|_{2,\infty} |\Delta|^2 + 2\|\epsilon\|_{\mathcal{P}} + \sqrt{\frac{1}{N}} \sqrt{\mathcal{E}_2(f)} \quad (51)$$

from Theorem 11. Thus,

$$\|\hat{F}_n - f\|_{\mathcal{P}} \leq \|M\hat{\mathbf{x}} - \mathbf{f}\|_{\mathcal{P}} \leq \sqrt{r} \|\delta\|_{\mathcal{P}} + \|\delta\|_{\mathcal{P}}. \quad (52)$$

When f is Kolmogorov-Lipschitz continuous with Lipschitz constant L , we know $\epsilon = O(L/n)$ from Corollary 1. Combining the estimate in (51), we have

$$\|\hat{F}_n - f\|_{\mathcal{P}} \leq (\sqrt{r} + 1)C\|f\|_{2,\infty}|\Delta|^2 + O((\sqrt{r} + 1)L/n + \sqrt{\frac{2r}{N}}\sqrt{\mathcal{E}_2(f)}), \quad (53)$$

where r is the rank of X_{data} and is strictly less than nd . We can choose $|\Delta|$ so small to make $\sqrt{nd}|\Delta|^2$ small enough, e.g. $O(1/n^\alpha)$, $N \gg n$ such that $2r/N = O(nd/N) = O(1/n^{2\alpha})$ as well as $\sqrt{nd}/n = O(1/n^\alpha)$ with $n \gg \sqrt{d}$.

In addition to the equally-spaced points from $[0, 1]^d$, we can also use a set of randomized point locations over $[0, 1]^d$. The above approach can also be applied. Let us conclude all the discussion above and write down one of our main results in this paper.

Theorem 16 *For any $n \gg 1$, there exists a set \mathcal{D}_n of pivotal data locations over $[0, 1]^d$ with the cardinality $|\mathcal{D}_n| < nd$ such that for any $f \in C[0, 1]^d$, the discrete least squares problem (48) based on the function measurements $\mathbf{f}_I = [f(\mathbf{x}_i), \mathbf{x}_i \in \mathcal{D}_n]$ is solved to obtain a LKB spline \hat{F}_n . Then if $f \in C^2([0, 1]^d)$, the LKB spline \hat{F}_n approximates f very well in the sense of (52). Furthermore, if f is also Kolmogorov-Lipschitz continuous with Lipschitz constant L , then the LKB spline \hat{F}_n approximates f in the sense of (53).*

Let us call the data locations associated with row indices I the pivotal data locations. Also, we will call such data locations magic data locations. Two examples of pivotal data locations are shown in Figure 6. It is worthwhile to point out that such a set of pivotal locations is only dependent on the knot partition of $[0, d]$ when numerically building KB-splines, the sampled data when constructing LKB-splines, and the smoothing parameters for converting KB-splines to LKB-splines. However, such a set of pivotal locations is independent of any testing functions or the target function to approximate.

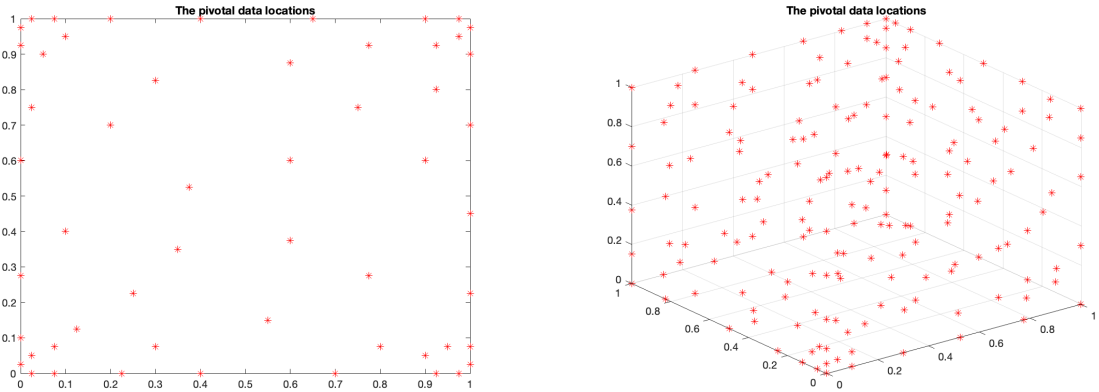


Figure 6: Pivotal data at 54 locations (selected from 41^2 equally-spaced locations) in 2D and 178 locations (selected from 41^3 equally-spaced locations) in 3D for $n = 100$.

The above discussion shows that we only need to nd LKB-splines $LKB_{n,j}, j = 1, \dots, nd$ and the measurement of any function f over a set of pivotal data locations with the number of the pivotal data location set less than nd to obtain LKB-spline approximation \hat{F}_n of f over a dense set over $[0, 1]^d$ with a number $N \gg nd$. These finish our approach to approximate smooth continuous functions in the multi-dimensional setting. This approach does not suffer from the curse of dimensionality although the computation of the denoising process to obtain LKB-splines will take a lot of computer power when

$d \gg 2$. Nevertheless, $LKB_{n,j}, j = 1, \dots, nd$ can be computed independently and the measurements of the values from $KB_{n,j}, j = 1, \dots, nd$ are obtained based on their computation. Essentially, we need some big companies like Google and Microsoft to help us obtain these LKB-splines B_{nj} when $d \gg 2$. The rest of us can simply use them to approximate any Kolgoromov-Lipschitz continuous functions without the curse of dimensionality.

5.3 Numerical Approximation by LKB-splines

For the numerical experiments, we choose 41^d equally-spaced points $\mathbf{x}_i \in [0, 1]^d$. For any continuous function $f \in C([0, 1]^d)$, we first use the function values at these data locations to experiment an approximation $F_n = \sum_{j=1}^{dn} c_j LKB_{n,j}$ by using discrete least squares (DLS) method via (39). Then we use the pivotal data locations to interpolate the given function values at these data locations. We will show the convergence in the RMS semi-norm over 101^d equally-spaced points in $[0, 1]^d$. The current computational power enables to do the numerical experiments for $d = 2$ with $n = 100, 200, \dots, 10,000$ and for $d = 3$ with $n = 100, 200, \dots, 1000$.

For $d = 2$, we choose the following 10 testing functions across different families of continuous functions to check the computational accuracy. They are among 100 testing functions we have experimented so far.

$$\begin{aligned} f_1 &= (1 + 2x + 3y)/6; & f_2 &= (x^2 + y^2)/2; & f_3 &= xy; \\ f_4 &= (x^3 + y^3)/2; & f_5 &= 1/(1 + x^2 + y^2); \\ f_6 &= \cos(1/(1 + xy)); & f_7 &= \sin(2\pi(x + y)); \\ f_8 &= \sin(\pi x) \sin(\pi y); & f_9 &= \exp(-x^2 - y^2); \\ f_{10} &= \max(x - 0.5, 0) \max(y - 0.5, 0); \end{aligned}$$

Table 1: RMSEs (computed based on 101^2 equally-spaced locations) of the DLS fitting (39) based on 41^2 equally-spaced location and pivotal location in 2D.

# sampled data	$n = 100$		$n = 1000$		$n = 10000$	
	41^2	54	41^2	105	41^2	521
f_1	1.67e-05	2.60e-05	5.79e-06	1.02e-05	5.14e-07	1.21e-06
f_2	4.19e-04	8.92e-04	1.17e-04	2.61e-04	2.83e-05	6.62e-05
f_3	1.09e-04	2.19e-04	3.57e-05	7.46e-05	2.20e-05	5.67e-05
f_4	7.67e-04	1.70e-03	2.10e-04	5.11e-04	4.99e-05	1.11e-04
f_5	2.28e-04	5.04e-04	6.69e-05	1.47e-04	1.93e-05	4.08e-05
f_6	2.52e-04	6.51e-04	7.97e-05	1.94e-04	1.43e-05	2.73e-05
f_7	7.05e-02	1.32e-01	7.80e-03	2.25e-02	1.30e-03	3.30e-03
f_8	1.50e-03	2.29e-03	3.73e-04	1.01e-03	1.69e-04	4.37e-04
f_9	3.49e-04	7.97e-04	8.25e-05	1.98e-04	2.48e-05	5.52e-05
f_{10}	2.02e-03	3.79e-03	7.77e-04	1.82e-03	1.68e-04	4.10e-04

For $d = 3$, we choose the following 10 testing functions across different families of continuous functions to check the computational accuracy. In fact we have tested more than 100 testing functions. The computational results are reported in Tables 1 and 2 (those columns associated with 41^3).

$$\begin{aligned} f_1 &= (1 + 2x + 3y + 4z)/10; & f_2 &= (x^2 + y^2 + z^2)/3; & f_3 &= (xy + yz + zx)/3; \\ f_4 &= (x^3y^3 + y^3z^3)/2; & f_5 &= (x + y + z)/(1 + x^2 + y^2 + z^2); \end{aligned}$$

$$\begin{aligned}
f_6 &= \cos(1/(1 + xyz)); & f_7 &= \sin(2\pi(x + y + z)); \\
f_8 &= \sin(\pi x) \sin(\pi y) \sin(\pi z); & f_9 &= \exp(-x^2 - y^2 - z^2); \\
f_{10} &= \max(x - 0.5, 0) \max(y - 0.5, 0) \max(z - 0.5, 0);
\end{aligned}$$

We now present the numerical results in Table 1 and 2 to demonstrate that the numerical approximation results based on pivotal data locations (those columns associated with 54, 105, 521 (in Table 1) and 178, 331, 643 (in Table 2) have the same order as the results based on data locations sampled on the uniform grid with 41^d locations. We therefore conclude that the curse of dimensionality for 2D and 3D function approximation is broken if we use LKB-splines with pivotal data locations.

Table 2: RMSEs (computed based on 101^3 equally-spaced locations) of the DLS fitting (39) based on 41^3 equally-spaced location and pivotal location in 3D.

	$n = 100$		$n = 300$		$n = 1000$	
# sampled data	41^3	178	41^3	331	41^3	643
f_1	8.27e-06	2.25e-05	1.51e-06	4.20e-06	3.62e-07	7.48e-07
f_2	4.42e-05	1.68e-04	8.14e-06	2.18e-05	1.87e-06	4.11e-06
f_3	1.24e-05	3.79e-05	3.77e-06	9.41e-06	1.22e-06	2.53e-06
f_4	2.93e-04	5.60e-04	1.43e-04	2.55e-04	1.16e-04	2.63e-04
f_5	1.31e-04	3.46e-04	9.09e-05	1.66e-04	6.61e-05	1.20e-04
f_6	1.24e-04	3.22e-04	7.02e-05	1.34e-04	5.18e-05	1.09e-04
f_7	1.65e-02	5.29e-02	1.15e-02	1.71e-02	1.10e-02	1.85e-02
f_8	2.47e-03	8.28e-03	9.60e-04	1.94e-03	7.20e-04	1.19e-03
f_9	1.43e-04	3.84e-04	1.14e-04	2.01e-04	9.84e-05	3.95e-04
f_{10}	3.21e-04	9.74e-04	2.31e-04	4.00e-04	2.04e-04	3.91e-04

Remark 2 *The major computational burden for the results in Tables 1 and 2 is the denoise of the KB-splines to get LKB-splines which requires a large amount of data points and values as the noises are everywhere over $[0, 1]^d$. When dimension $d \gg 2$ gets large, one has to use an exponentially increasing number of points and KB-spline values by, say a tensor product spline method for denoising, and hence, the computational cost will suffer the curse of dimensionality. However, the denoising step can be pre-computed once for all and can be done in parallel. In particular, obtaining these large amount of data values is done by computation. That is, once we have the LKB-splines, the rest of the computational cost is no more than the cost of solving a least squares problem. We leave the numerical results for $d > 3$ in [63] and [41].*

To verify the approximation order $O(1/n)$ in Theorem 6, we plot the approximation errors of several aforementioned functions based on pivotal point locations against n using log-log scale. The results are shown in Figure 7. It is worthwhile to note that the slopes in these plots are associated with the exponent α in Theorem 7. In other words, if the slope of an convergence plot for a function is smaller than -1 , then we can numerically conclude that such a function belongs to the KL class. If the slope α satisfies $-1 < \alpha < 0$, then we can numerically conclude that such a function belongs to KH class as the outer function g belongs to $C^{0,\alpha}$. In other words, our computational method provides a numerical approach to check if a multidimensional continuous function is KL or not.

Finally, in Figure 8, we plot the number of pivotal locations against n , we can see that the number of pivotal locations increasing linearly with n and the increasing rates (slopes) are at most d .

That is, we only need $O(nd)$ data locations and $O(nd)$ LKB functions to approximate a multidimensional continuous function f with approximation rate $O(1/n)$ when f is KL. Therefore, the curse of dimensionality is overcome when $d = 2$ and $d = 3$. See [63] for numerical evidence for $d = 4, 5, 6$.

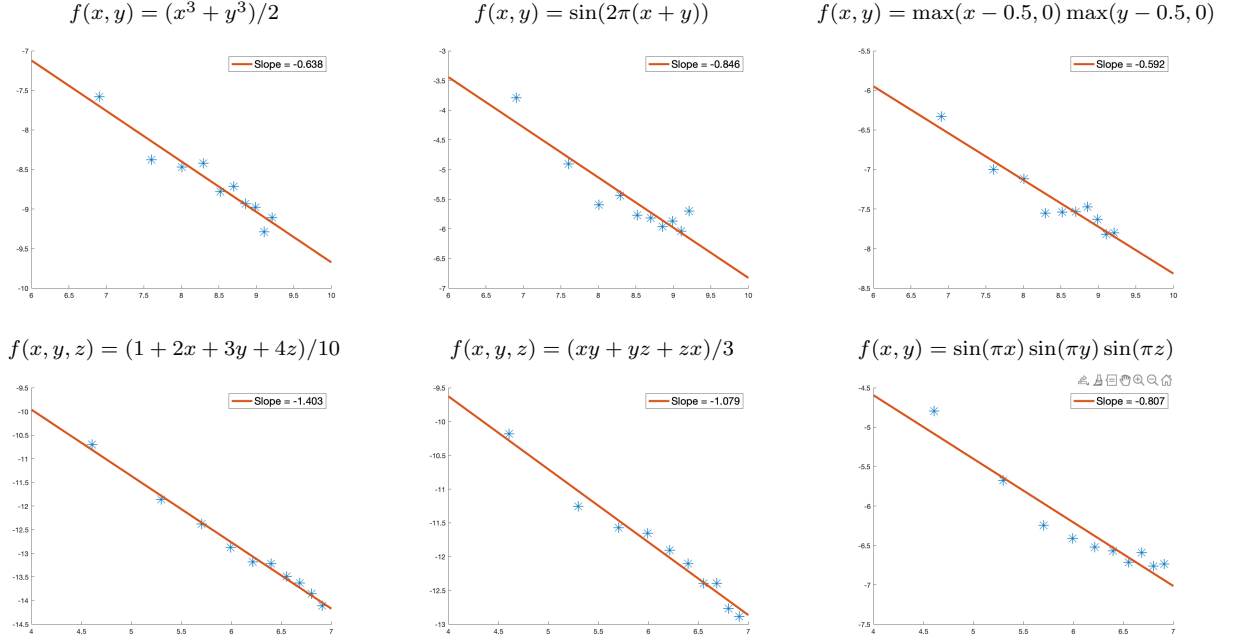


Figure 7: Plot of Convergence Rate using Log-log Scale for Functions in 2D and 3D.

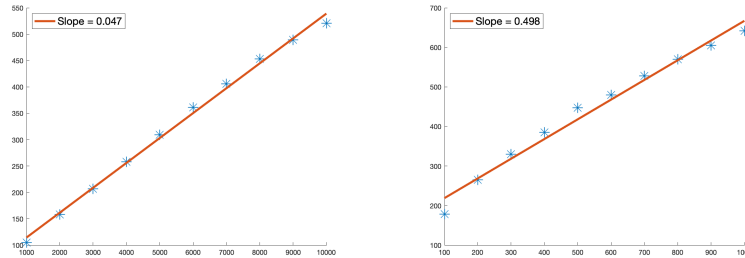


Figure 8: Number of Pivotal Locations (vertical axis) against n (horizontal axis) in 2D (left) and in 3D (right).

Finally, let us end up this section with some important remarks.

Remark 3 *The pivotal data set is independent of the degree of KB-splines and the LKB-splines which are dependent on the smoothing parameters and triangulation for converting KB-splines to LKB-splines. After LKB-splines are constructed, the pivotal point set is dependent on the discrete least squares (DLS) fitting method. For example, if we use randomly sampled points over $[0, 1]^d$ for a DLS method instead of equally-space points, the pivotal point set is clearly different from the pivotal points based on the equally-spaced points over $[0, 1]^d$. Even if we use 81×81 equally-spaced points instead of 41×41 equally-spaced points when constructing a DLS fitting based on LKB-splines over $[0, 1]^2$, the location of the pivotal data are different and the size of pivotal data set is slightly bigger than the ones shown in Figure 6. Although we can apply this trick to find a pivotal point set for any discrete least*

squares method, it is the K -outer function g defined on $[0, d]$ which enables us to approximate the g using nd LKB-splines based on the pivotal point set with cardinality at most nd to achieve the rate $O(1/n)$ of approximation.

Remark 4 Certainly, there are many functions such as $f(x, y) = \sin(100x)\sin(100y)$ or $f(x, y) = \tanh(100((2x - 1)^2 + (2y - 1)^2 - 0.25))$ which the LKB-splines can not approximate well based on the pivotal data sets above. Such highly oscillated functions are hard to approximate even using other methods. We believe that these functions will have a large Kolmogorov-Lipschitz constant. One indeed needs a lot of the data (points and the function values over the points) in order to approximate them well. One may also consider to use Fourier basis as K -outer functions rather than B -splines basis to approximate such highly oscillated trigonometric functions via KST. We leave it as a future research topic.

Remark 5 To reproduce the experimental results in this paper, we uploaded our MATLAB codes in <https://github.com/zzzzms/KST4FunApproximation>. In fact, we have tested more than 100 functions in 2D and 3D with pivotal data sets which enables us to approximate these functions very well.

Acknowledgement:

The authors would like to thank the anonymous reviewers for their comments and suggestions which improve the readability of the paper.

References

- [1] K. Allen, M.-J. Lai, and Z. Shen. Maximal volume matrix cross approximation for image compression and least squares solution. *Advances in Computational Mathematics* 50, no. 5 (2024): 102.
- [2] G. Awanou, M.-J. Lai, P. Wenston, The multivariate spline method for scattered data fitting and numerical solutions of partial differential equations, *Wavelets and splines: Athens* (2005), 24–74.
- [3] F. Bach, Breaking the curse of dimensionality with convex neural networks, *Journal of Machine Learning Research*, vol. 18, 2017, 1–53.
- [4] A. R. Barron. Universal approximation bounds for superpositions of a sigmoidal function, *IEEE Transactions on Information theory*, 39(3):930–945, 1993.
- [5] B. J. Braun, An Application of Kolmogorov’s Superposition Theorem to Function Reconstruction in Higher Dimensions, PhD thesis, University of Bonn, 2009.
- [6] B. J. Braun and M. Griebel, On a constructive proof of Kolmogorov’s superposition theorem, *Constructive Approximation*, 30(3):653–675, 2009.
- [7] D. W. Bryant. Analysis of Kolmogorov’s superposition theorem and its implementation in applications with low and high dimensional data. PhD thesis, University of Central Florida, 2008
- [8] K. Chen, The upper bound on knots in neural networks, arXiv preprint arXiv:1611.09448 (2016)
- [9] E. W. Cheney, *Approximation Theory*, AMS Publication, Chelsea, 1998.
- [10] G. Cybenko, Approximation by Superpositions of a Sigmoidal Function, *Math. Control Signals Systems* (1989) 2:303–314.

- [11] I. Daubechies, R. DeVore, S. Foucart, B. Hanin, and G. Petrova, Nonlinear Approximation and (Deep) ReLU Networks, *Constructive Approximation* 55, no. 1 (2022): 127-172.
- [12] R. DeVore, R. Howard, and C. Micchelli, Optimal nonlinear approximation, *Manuscripta Mathematica*, 63(4):469–478, 1989.
- [13] R. DeVore, B. Hanin, and G. Petrova, Neural Network Approximation, *Acta Numerica* 30 (2021): 327-444.
- [14] R. Doss, On the representation of continuous functions of two variables by means of addition and continuous functions of one variable. *Colloquium Mathematicum*, X(2):249–259, 1963.
- [15] Weinan E, Machine Learning and Computational Mathematics, arXiv:2009.14596v1 [math.NA] 23 Sept. 2020.
- [16] Weinan E, Chao Ma and Lei Wu, Barron spaces and the flow-induced function spaces for neural network models, *Constructive Approximation* 55, no. 1 (2022): 369-406
- [17] Weinan E and Stephan Wojtowytsch, Representation formulas and pointwise properties for Barron functions, *Calculus of Variations and Partial Differential Equations* 61, no. 2 (2022): 1-37.
- [18] Weinan E and Stephan Wojtowytsch, On the Banach spaces associated with multilayer ReLU networks: Function representation, approximation theory and gradient descent dynamics, <https://arxiv.org/abs/2309.17403>
- [19] D. Fakhoury, E. Fakhoury, and H. Speleers, ExSpliNet: An interpretable and expressive spline-based neural network, *Neural Networks* 152, pp. 332–346, 2022.
- [20] B. L. Friedman, An improvement in the smoothness of the functions in Kolmogorov’s theorem on superpositions. *Doklady Akademii Nauk SSSR*, 117:1019–1022, 1967.
- [21] Z. Feng, Hilbert’s 13th problem. PhD thesis, University of Pittsburgh, 2010.
- [22] Irina Georgieva and Clemens Hofreithery, On the Best Uniform Approximation by Low-Rank Matrices, *Linear Algebra and its Applications*, vol.518(2017), Pages 159–176.
- [23] Girosi, F., and Poggio, T. (1989). Representation properties of networks: Kolmogorov’s theorem is irrelevant. *Neural Computation*, 1(4), 465-469.
- [24] I. Goodfellow, Y. Bengio, A. Courville, *Deep Learning*, MIT Press, 2016.
- [25] S. A. Goreinov and E. E. Tyrtysnikov, The maximal-volume concept in approximation by low-rank matrices, *Contemporary Mathematics*, 208: 47–51, 2001.
- [26] S. A. Goreinov, I. V. Oseledets, D. V. Savostyanov, E. E. Tyrtysnikov, N. L. Zamarashkin, How to find a good submatrix, in: *Matrix Methods: Theory, Algorithms, Applications*, (World Scientific, Hackensack, NY, 2010), pp. 247–256.
- [27] N. Kishore Kumar and J. Schneider, Literature survey on low rank approximation of matrices, *Journal on Linear and Multilinear Algebra*, vol. 65 (2017), 2212–2244.
- [28] M. Hansson and C. Olsson, Feedforward neural networks with ReLU activation functions are linear splines, Bachelor Thesis, Univ. Lund, 2017.

- [29] R. Hecht-Nielsen, Kolmogorov’s mapping neural network existence theorem. In Proceedings of the international conference on Neural Networks, volume 3, pages 11–14. New York: IEEE Press, 1987.
- [30] K. Hornik, Approximation capabilities of multilayer feedforward networks. *Neural Networks* 4, no. 2 (1991): 251–257.
- [31] B. IgelNIK and N. Parikh, Kolmogorov’s spline network. *IEEE Transactions on Neural Networks*, 14(4):725–733, 2003.
- [32] J. M. Klusowski and Barron, A.R.: Approximation by combinations of ReLU and squared ReLU ridge functions with ℓ_1 and ℓ_0 controls. *IEEE Transactions on Information Theory* 64(12), 7649–7656 (2018).
- [33] A. N. Kolmogorov. The representation of continuous functions of several variables by superpositions of continuous functions of a smaller number of variables. *Doklady Akademii Nauk SSSR*, 108(2):179–182, 1956.
- [34] A. N. Kolmogorov, On the representation of continuous function of several variables by superposition of continuous function of one variable and its addition, *Dokl. Akad. Nauk SSSR* 114 (1957), 369–373.
- [35] V. Kurkov, Kolmogorov’s Theorem and Multilayer Neural Networks, *Neural Networks*, Vol. 5, pp. 501– 506, 1992.
- [36] M.-J. Lai, Multivariate splines for Data Fitting and Approximation, the conference proceedings of the 12th Approximation Theory, San Antonio, Nashboro Press, (2008) edited by M. Neamtu and Schumaker, L. L. pp. 210–228.
- [37] M.-J. Lai and J. Lee, A multivariate spline based collocation method for numerical solution of partial differential equations, *SIAM J. Numerical Analysis*, vol. 60 (2022) pp. 2405–2434.
- [38] M.-J. Lai and L. L. Schumaker, *Spline Functions over Triangulations*, Cambridge University Press, 2007.
- [39] M.-J. Lai and L. L. Schumaker, Domain Decomposition Method for Scattered Data Fitting, *SIAM Journal on Numerical Analysis*, vol. 47 (2009) pp. 911–928.
- [40] M.-J. Lai and Wang, L., Bivariate penalized splines for regression, *Statistica Sinica*, vol. 23 (2013) pp. 1399–1417.
- [41] M.-J. Lai and Z. Shen. The Optimal Rate for Linear KB-splines and LKB-splines Approximation of High Dimensional Continuous Functions and its Application. *Sampling Theory, Signal Processing, and Data Analysis*. Accepted with minor Revision, 2024.
- [42] M.-J. Lai and Y. Wang, *Sparse Solutions of Underdetermined Linear Systems and Their Applications*, SIAM Publication, 2021.
- [43] M. Laczkovich, A superposition theorem of Kolmogorov type for bounded continuous functions, *J. Approx. Theory*, vol. 269(2021), 105609.
- [44] Ziming Liu, Yixuan Wang, Sachin Vaidya, Fabian Ruehle, James Halverson, Marin Soljačić, Thomas Y. Hou, Max Tegmark, KAN: Kolmogorov-Arnold Networks, *arXiv preprint arXiv:2404.19756* (2024).

- [45] X. Liu, Kolmogorov Superposition Theorem and Its Applications, Ph.D. thesis, Imperial College of London, UK, 2015.
- [46] J. Lu, Z. Shen, H. Yang, S. Zhang, Deep Network Approximation for Smooth Functions, SIAM Journal on Mathematical Analysis, 2021.
- [47] G. G. Lorentz, Metric entropy, widths, and superpositions of functions, Amer. Math. Monthly, 69 (1962), 469–485.
- [48] G. G. Lorentz, Approximation of Functions, Holt, Rinehart and Winston, Inc. 1966.
- [49] V. E. Maiorov, On best approximation by ridge functions, J. Approx. Theory 99 (1999), 68–94.
- [50] V. Maiorov and A. Pinkus, Lower bounds for approximation by MLP neural networks, Neurocomputing, 25 (1999), pp. 81–91.
- [51] S. Mallat, Understanding Deep Convolutional Network, Philosophical Transactions A, in 2016.
- [52] H. Mhaskar, C. A. Micchelli, Approximation by superposition of sigmoidal and radial basis functions, Adv. Appl. Math. 13 (3) (1992) 350–373.
- [53] A. Mikhaleva and I. V. Oseledets, Rectangular maximum-volume submatrices and their applications, Linear Algebra and its Applications, Vol. 538, 2018, Pages 187–211.
- [54] H. Montanelli and H. Yang, Error Bounds for Deep ReLU Networks using the Kolmogorov–Arnold Superposition Theorem. Neural Networks, 2020.
- [55] H. Montanelli, H. Yang, Q. Du, Deep ReLU Networks Overcome the Curse of Dimensionality for Bandlimited Functions. Journal of Computational Mathematics, 2021.
- [56] S. Morris, Hilbert 13: are there any genuine continuous multivariate real-valued functions? Bulletin of AMS, vol. 58. No. 1 (2021), pp 107–118.
- [57] A. Pinkus, Approximation theory of the MLP model in neural networks, Acta Numerica (1999), pp. 143–195.
- [58] P. P. Petrushev, Approximation by ridge functions and neural networks, SIAM J. Math. Anal. 30 (1998), 155–189.
- [59] M. J. Powell, Approximation theory and methods, Cambridge University Press, 1981.
- [60] J. Schmidt-Hieber, The Kolmogorov–Arnold representation theorem revisited. Neural Networks, 137 (2021), 119–126.
- [61] L. L. Schumaker, Spline Functions: Basic Theory, Third Edition, Cambridge University Press, 2007.
- [62] L. L. Schumaker, Spline Functions: Computational Methods, SIAM Publication, Philadelphia (2015),
- [63] Z. Shen, Sparse Solution Technique in Semi-supervised Local Clustering and High Dimensional Function Approximation. Ph.D. Dissertation, University of Georgia, 2024.
- [64] Z. Shen, H. Yang, S. Zhang. Neural Network Approximation: Three Hidden Layers Are Enough. Neural Networks, 2021.

- [65] Z. Shen, H. Yang, and S. Zhang, Deep Network Approximation: Achieving Arbitrary Accuracy with Fixed Number of Neurons. *Journal of Machine Learning Research*, 2022.
- [66] J. W. Siegel and J. Xu, Approximation rates for neural networks with general activation functions, *Neural Networks* 128 (2020): 313-321.
- [67] J. W. Siegel and J. Xu. High-Order Approximation Rates for Shallow Neural Networks with Cosine and $(ReLU)^k$ Activation Functions, *Applied and Computational Harmonic Analysis* 58 (2022): 1-26.
- [68] Sho Sonoda and Noboru Murata, Neural network with unbounded activation functions is universal approximator, *Applied and Computational Harmonic Analysis* 43, no. 2 (2017): 233-268.
- [69] D. A. Sprecher, Ph.D. Dissertation, University of Maryland, 1963.
- [70] D. A. Sprecher, A representation theorem for continuous functions of several variables, *Proc. Amer. Math. Soc.* 16 (1965), 200–203.
- [71] D. A. Sprecher, On the structure of continuous functions of several variables. *Transactions of the American Mathematical Society*, 115:340–355, 1965.
- [72] D. A. Sprecher, On the structure of representation of continuous functions of several variables as finite sums of continuous functions of one variable. *Proceedings of the American Mathematical Society*, 17(1):98–105, 1966.
- [73] D. A. Sprecher, An improvement in the superposition theorem of Kolmogorov. *Journal of Mathematical Analysis and Applications*, 38(1):208–213, 1972.
- [74] D. A. Sprecher, A universal mapping for Kolmogorov’s superposition theorem. *Neural Networks*, 6(8):1089–1094, 1993.
- [75] D. A. Sprecher, A numerical implementation of Kolmogorov’s superpositions. *Neural Networks*, 9(5):765–772, 1996.
- [76] D. A. Sprecher, A Numerical Implementation of Kolmogorov’s Superpositions II. *Neural Networks*, 10(3):447–457, 1997.
- [77] M. Von Golitschek, Lai, M. -J. and Schumaker, L. L., Bounds for Minimal Energy Bivariate Polynomial Splines, *Numerisch Mathematik*, vol. 93 (2002) pp. 315–331.
- [78] L. Wang, G. Wang, M. -J. Lai, and Gao, L., Efficient Estimation of Partially Linear Models for Spatial Data over Complex Domains, *Statistica Sinica*, vol. 30 (2020) pp. 347–360.
- [79] D. Yarotsky, Error bounds for approximations with deep ReLU networks, *Neural Networks* 94 (2017): 103-114.
- [80] D. Yarotsky and A. Zhevnerchuk, The phase diagram of approximation rates for deep neural networks, *Advances in neural information processing systems* 33 (2020): 13005-13015.